

# NUMERICAL ACCURACY OF NOP SDS2 DETECTORS DYNAMIC COMPENSATION IN DARLINGTON TRIP COMPUTERS

A.P. Firla, Nuclear Analysis Dept., SESD, Ontario Hydro, Toronto.  
June 1998.

## Abstract

In Darlington reactors' SDS2 safety systems the self-powered NOP detectors of platinum-clad inconel type are used. Such detectors are characterized by underprompt, lagging response to neutron flux and therefore have to be dynamically compensated. The SDS2 NOP compensation is realized digitally, utilizing a backward finite difference numerical algorithm resident in the SDS2 trip computers. Four dynamic first order lag terms, designated in this paper as  $C_j(t)$ ,  $j = 1, \dots, 4$ , are used for the dynamic compensation task, with time constants  $\tau_j$  ranging from 30 sec up to 300,000 sec. The dynamic terms  $C_j(t)$  are numerically computed by the compensation algorithm with sampling times  $\Delta T_j$  ranging correspondingly from 3 sec to 3000 sec. Because of the final difference form and the four different sampling times used in the algorithm, a dynamic numerical compensation error  $\epsilon(t)$  occurs. The error  $\epsilon(t)$  is evaluated by comparing the numerically compensated detector response  $DtCmp\_alg(t_k)$  with the "ideally" compensated detector response  $DtCmp(t)$  provided by continuous, analytical solution of compensator mathematical model. The continuous response  $DtCmp(t)$  is calculated analytically, separately for the bounded ramp-type and the step-type changes in neutronic power. The numerical compensation algorithm is emulated and the compensator's numerical error  $\epsilon(t)$  is calculated as

$$\epsilon(t) = DtCmp(t) - DtCmp\_alg(t), \quad t \in [0, T];$$

utilizing a specially developed simulation code DACER. The resulting magnitudes and shape of the error transient  $\epsilon(t)$  strongly depend on the relative timing of the first simultaneous action of the four compensating terms  $C_j(t)$ , with respect to the initiation moment  $t_0$  of the neutronic power change.

Results of computations of the compensator numerical error  $\epsilon(t)$  calculated for a family of ramp and step-type transients in neutronic power are presented and discussed. The resulting bounds for the short term compensation error (less than 300 sec duration time) and the long term error (beyond 300 sec duration time) are shown.

## 1. Introduction

In Darlington reactors' SDS2 NOP safety systems the straight individually replaceable (SIR), self-powered detectors (SPDs) of platinum-clad inconel type are used. The theory and properties of SPD detectors, including the platinum-clad inconel detectors' dynamic response, are described in Ref.1. In general, the net current  $I$  from an SPD can be described as a sum of four distinct components

$$I = I_{(n,\gamma,e)} + I_{(n,\beta)} + I_{(\gamma,e)} + I_{(e)}; \quad (1)$$

where:  $I_{(n,\gamma,e)}$  = Current due to electrons resulting from  $(n,\gamma,e)$  interactions in the detector,  
 $I_{(n,\beta)}$  = Current due to electrons resulting from  $(n,\beta)$  interactions,  
 $I_{(\gamma,e)}$  = Current due to electrons resulting from  $(\gamma,e)$  interactions (with gamma emitted from within the reactor core, external to the detector),  
 $I_{(e)}$  = Current due to electrons resulting from  $(n,\gamma,e)$ ,  $(n,\beta)$  and  $(\gamma,e)$  interactions in the hardware immediately surrounding the detector.

The  $I_{(e)}$  component is negative and small. The polarity and magnitude of the remaining three components depend mainly on construction, materials and diameters of the detector's emitter, insulator and collector. The relative magnitudes of these four components determine the dynamic response of the detector.

The NOP SDS2 platinum-clad inconel detectors are characterized by the underprompt, lagging response to neutron flux and therefore have to be dynamically compensated. As explained in Ref.1, the dynamic response of these detectors to neutron flux can be approximated by a model with constant prompt term

$F_p$  and a combination of dynamic 1st-order lags representing the delayed response terms. In the Laplace transform form the underprompt detector response is described as

$$Dt(s) = \left[ F_p + \sum_{j=1}^k \frac{d_j}{1 + \tau_j s} \right] \cdot Flx(s) ; \quad (2)$$

where:  $Dt(s)$  = detector response,  
 $F_p$  = prompt response term (constant),  
 $d_j$  = amplitude (gain) of the  $j^{\text{th}}$  lag term,  
 $\tau_j$  = time constant of the  $j^{\text{th}}$  lag term,  
 $Flx(s)$  = neutron flux,  
 $k$  = number of delayed (lag) terms in detector model.

The term in the brackets is the transfer function (see e.g. Ref.8) of the detector model. At the steady state, with normalized reactor power we have in time domain  $Dt(t) = Flx(t)$  and therefore  $[F_p + \sum_{j=1}^k d_j] = 1$ . The sum  $\sum_{j=1}^k d_j$  is positive, and hence the prompt detector response  $F_p$  to a sudden change in neutron power is initially smaller in magnitude (underprompt) than the actual change in neutron power. In Darlington SDS2-NOP Pt-clad Inconel detectors the "delayed" part represents about 8% of the total neutron power. As a result, the detector's initial response to a sudden increase (or decrease) in neutronic power amounts to about 92% of the actual change in total neutronic power. Then, gradually, the lagged part of the response begins to occur, governed by the lag time constants  $\tau_j, j = 1, \dots, k$  and the discrepancy between the detector reading and the actual reactor power decreases until, near the steady state, the detector reading becomes equal to reactor power.

To counteract the initial underprompt response and the transient discrepancy between the detector reading and the actual reactor power, the detector responses are dynamically compensated. The Laplace transform model of the compensator is given as

$$DtCmp(s) = \left[ \left( 1 + \sum_{j=1}^4 A_j \right) - \sum_{j=1}^4 \frac{A_j}{1 + \tau_j s} \right] \cdot Dt(s) ; \quad (3)$$

where:  $DtCmp(s)$  = compensated NOP detector response,  
 $A_j$  = magnitude of the  $j^{\text{th}}$  compensating lag component,  
 $\tau_j$  = time constant of the  $j^{\text{th}}$  compensating lag component,  
 $Dt(s)$  = (uncompensated) detector reading.

The compensator consists of the static term  $[1 + \sum_{j=1}^4 A_j]$  which compensates for the initial underprompt part of the detector response, and the four dynamic compensating terms in the form of first order lags designated in this paper as  $C_j(t), j = 1, \dots, 4$ . The dynamic terms  $C_j(t)$  compensate for the resulting transient discrepancy between the compensated detector reading and the actual reactor power. The time constants  $\tau_j$  range correspondingly from 30 sec up to 300,000 sec and the coefficients  $A_j, j = 1, \dots, 4$  have been chosen to compensate the detectors' signals and to ensure that the compensated detector response closely matches the fuel power.

The SDS2 NOP compensation algorithm corresponding to differential representation of the Laplace

transform model (3) is realized digitally in the SDS2 trip computers.

## 2. Methodology of Analysis

### 2.1 Notation, Definitions and Basic Assumptions

- $i$  = NOP detector index ;  
 $j$  = compensator lag term index ;  
 $s$  = Laplace transform variable (complex) ;  
 $t$  = time ;  
 $t_k$  = discrete time ;  
 $t_0 = 0$  = initial time moment ;  
 $t_{act}$  = time when the four compensating terms  $C_{alg_j}$  are triggered into action simultaneously for the first time (after  $t_0$ ) ;  
 $\eta_{act}$  =  $t_{act} - t_0$  = relative time of the first simultaneous compensating action, evaluated with respect to  $t_0$ ;  $\eta_{act}$  is a random variable ;  
 $\Delta t_j$  = time increment, used in the compensator numerical algorithm for sequential calculation of the  $j^{th}$  lag term ;  
 $a_j, A_j$  = gain coefficient in compensator's  $j^{th}$  lag term (for generic, unspecified detector) ;  
 $a_{i_j}, A_{i_j}$  = gain coefficient in compensator's  $j^{th}$  lag term (for the  $i^{th}$  detector) ;  
 $\tau_j$  = time constant in compensator's  $j^{th}$  lag term (for generic, unspecified detector) ;  
 $\tau_{i_j}$  = time constant in compensator's  $j^{th}$  lag term (for the  $i^{th}$  detector) ;  
 $C_j(t)$  = output of the compensator's  $j^{th}$  lag term (for generic, unspecified detector) ;  
 $C_j(t_0) = C_j^0$  = initial condition for  $C_j(t)$  ;  
 $SC(t) = \sum_{j=1}^4 C_j(t)$ , is a sum of all compensating lag terms (for a generic detector) ;  
 $Dt(t)$  = NOP detector uncompensated reading (for a generic detector) ;  
 $Dt_i(t)$  = NOP detector uncompensated reading (for the  $i^{th}$  detector) ;  
 $DtCmp(t)$  = compensated detector "ideal" response (for a generic detector), based on exact mathematical time-domain representation of Eq.(8) ;  
 $DtCmp_i(t)$  = compensated detector "ideal" response (for  $i^{th}$  detector), based on exact mathematical time-domain representation of Eq.(8) ;  
 $\Theta_{NP}(t)$  = simulated changes in neutronic power, represented by uncompensated, "perfectly prompt" NOP detector reading, used as an input in calculated compensator action ;  
 $b_0, b, a, D$  = parameters of simulated variations in neutronic power  $\Theta_{NP}(t)$  ;  
 $\| (t) = \begin{cases} 1 & \text{for } t > 0 ; \\ 0 & \text{for } t \leq 0 ; \end{cases}$  is the unit step function ;  
 $C_{alg_j}(t_k)$  = output of the compensator's  $j^{th}$  lag term (for generic, unspecified detector), calculated at discrete time  $t_k$  by the compensator numerical algorithm (5) ;  
 $C_{alg_j}(t_0) = C_{alg_j}^0$  = initial condition for  $C_{alg_j}(t_k)$  ;  
 $SC_{alg}(t_k) = \sum_{j=1}^4 C_{alg_j}(t_k)$ , sum of all compensating lag terms (for a generic detector), calculated at discrete time  $t_k$  by the compensator numerical algorithm (5) ;  
 $DtCmp_{alg}(t_k)$  = compensated detector response (for a generic detector), calculated at discrete time  $t_k$  by the SDS2 trip computer numerical algorithm (5) ;

$DtCmp\_alg_i(t_k)$  = compensated detector response (for  $i^{th}$  detector), calculated at discrete time  $t_k$  by the SDS2 trip computer numerical algorithm (5) ;

$DtCmp\_alg_i(t) = DtCmp\_alg_i(t_k)$  , for  $t_k \leq t < t_{k+1}$  ,  $k = 0, 1, 2, \dots$  ;

$\epsilon_i(t) \triangleq DtCmp_i(t) - DtCmp\_alg_i(t)$  = error of the compensator algorithm, calculated for  $i^{th}$  detector;

$\epsilon(t) \triangleq DtCmp(t) - DtCmp\_alg(t)$  = error of the compensator algorithm, calculated for a generic detector;

$STE(t) \triangleq \epsilon(t)$  ,  $0 \leq t \leq 300$  sec = short term error of the compensator algorithm ;

$LTE(t) \triangleq \epsilon(t)$  ,  $t > 300$  sec = long term error of the compensator algorithm.

**Basic Assumptions** : The following basic assumptions have been used:

(A1): Uncompensated detector readings  $Dt_i(t)$  are simulated in this study as "ideal" in the sense that they exactly (without any delay) represent postulated changes in neutronic power  $\Theta_{NP}(t)$ , i.e.

$$Dt_i(t) = \Theta_{NP}(t) , \quad i = 1, 2, \dots, 17, \quad \text{for } t \geq 0.$$

(A2): Compensated individual detectors' responses to a postulated change in neutronic power  $\Theta_{NP}(t)$ , calculated by the numerical compensator algorithm (5) are identical because the same algorithm is used; therefore

$$DtCmp\_alg_i(t_k) = DtCmp\_alg(t_k) , \quad \text{and } \epsilon_i(t) = \epsilon(t) ; \quad \text{for } i = 1, 2, \dots, 17.$$

(A3): At the start  $t_0 = 0$  of a (simulated) compensator transient the reactor is at steady state with a specified power level.

(A4): No SDS2 trip computer failure is taken into account in the analysis, i.e. it is assumed that the NOP compensation algorithm is executed properly, without interruptions by the computer, and the proper initial conditions  $C\_alg_{ij}(t_0 = 0) = C_{ij}^0$  are used.

The assumption (A4) is justified by the objective of this analysis, which is to analyze and evaluate the compensation error introduced by the use of the numerical compensation algorithm alone, instead of the continuous operational amplifier-type representation. Also, in the safety analysis, dual process failures are considered but no simultaneous trip computer failure is postulated, because the probability of occurrence of such a multiple-failure event is very small.

As a consequence of assumptions (A1) and (A2), the foregoing analysis has been carried out for a single, generic SDS2 NOP detector and the results are applicable to the all 17 (per channel) SDS2 detectors.

## 2.2 Differential Model of the SDS2 NOP Dynamic Compensator

The compensator Laplace transform model described by Eq.(3) is referred to as the **mathematical reference model** of the compensator.

The values of the compensator parameters used in the reference model are summarized in Table 1 below. The same values of gain coefficients  $A_j$  and time constants  $\tau_j$  ,  $j = 1, \dots, 4$  are used in both the model's analytical solution and in the compensator numerical algorithm used in SDS2 trip computers. The last column of Table 1 gives the sampling times  $\Delta t_j$  used in the compensator numerical algorithm for periodic sampling of the individual compensating lag term loops. Observe that the sum of individual gains is equal to  $A_1 + \dots + A_4 = 0.066$  .

**Table 1.** Parameters of SDS2-NOP Detector Compensator

Lag term gain coefficient $A_j$	Time constant $\tau_j$	Corresponding sampling time $\Delta t_j$
$A_1 = 0.012$	$\tau_1 = 30 \text{ sec}$	$\Delta t_1 = 3 \text{ sec}$
$A_2 = 0.016$	$\tau_2 = 300 \text{ sec}$	$\Delta t_2 = 30 \text{ sec}$
$A_3 = 0.030$	$\tau_3 = 2400 \text{ sec}$	$\Delta t_3 = 300 \text{ sec}$
$A_4 = 0.008$	$\tau_4 = 300,000 \text{ sec}$	$\Delta t_4 = 3000 \text{ sec}$

It implies that the compensated response to a unit step-type change in neutronic power  $\Theta_{NP}(t)$ , from 0% to 100% FP, read by the "ideal" detector, such that  $Dt(t) = \Theta_{NP}(t)$ , will initially jump from 0% to 106.6% FP. After that, it will gradually decrease back to 100% FP, as the exponential responses of the individual compensating lag terms begin to subtract from the initial response term  $(1 + \sum_{j=1}^4 A_j)$ . The block diagram of the compensator reference model (3) is shown in Fig.1 below.

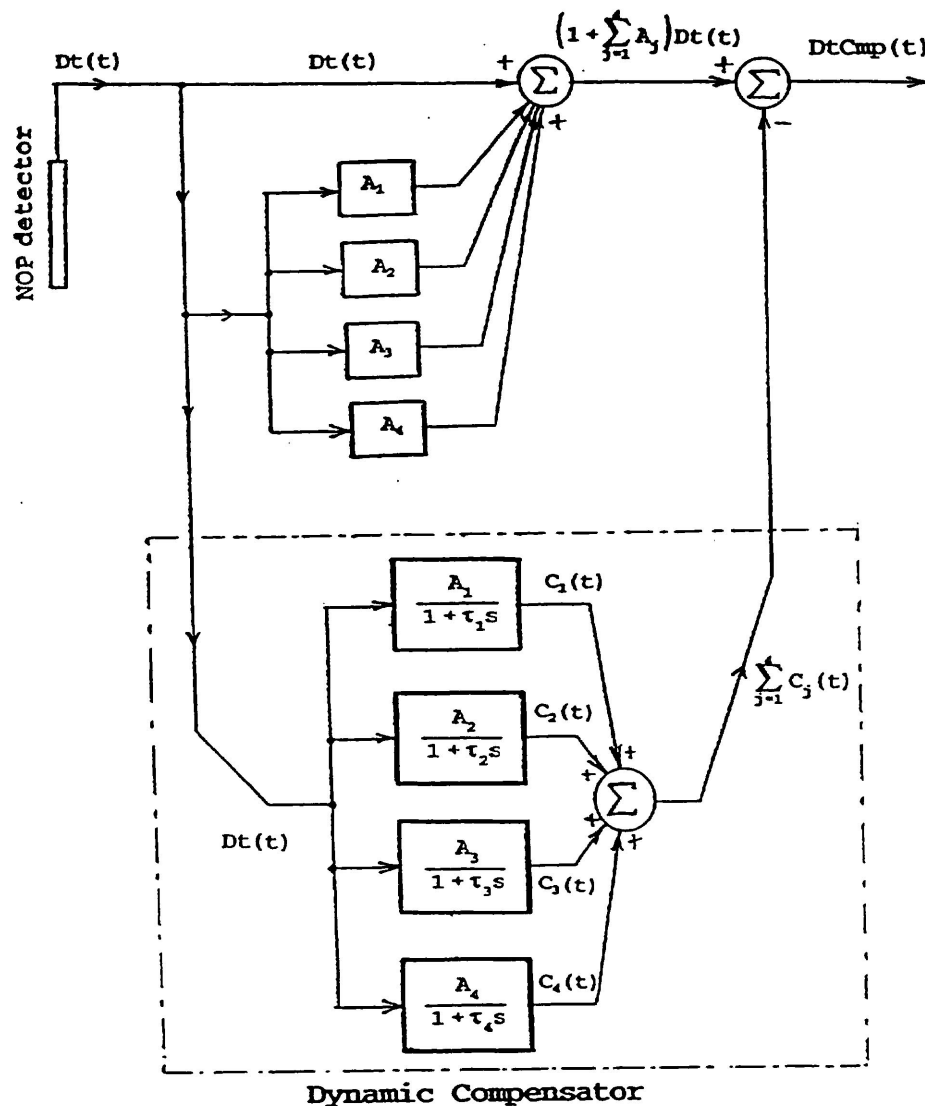


**Figure 1.** Block Diagram of the SDS2 NOP Detector Compensator Model

In the time-domain the compensator's Laplace transform model (3) is represented, (see e.g. Ref.9), by the following system (4) of first order linear differential equations, referred to in the text as the compensator's **differential model**.

$$\begin{aligned} \frac{dC_j(t)}{dt} &= -\frac{1}{\tau_j} \cdot C_j(t) + \frac{A_j}{\tau_j} \cdot Dt(t) ; & \dots\dots\dots (4) \\ C_j(t_0) &= C_j^0, t_0 = 0, j = 1, \dots, 4 \text{ are initial conditions ;} \\ SC(t) &= \sum_{j=1}^4 C_j(t) ; \\ DtCmp(t) &= (1 + \sum_{j=1}^4 A_j) \cdot Dt(t) - SC(t), t \geq t_0 ; \end{aligned}$$

where:  $Dt(t) = \Theta_{NP}(t)$  is the neutronic power read by an "ideal" detector.

The system (4) is representative for a generic SDS2 NOP detector, hence the detector index "i" is omitted. Solutions to the differential model (4) depend on the type of driving force  $Dt(t)$  and the initial conditions  $C_j^0, j = 1, \dots, 4$ . In particular, the lag term solutions  $C_j(t), j = 1, \dots, 4$ ; to the differential model (4) are uniquely defined by the initial conditions  $C_j^0$ . We assume that the reactor is initially at steady state, at initial power level  $b_0$ . Assuming proper operation of the compensator algorithm, the initial conditions  $C_j^0, j = 1, \dots, 4$ ; must be set in such a way that the compensated detector response  $DtCmp(t)$  calculated by the model (4), **matches exactly** the reactor steady state power  $b_0$ .

Analytical solutions to model (4) for step-type and bounded ramp-type variations in neutronic power driving force  $\Theta_{NP}(t)$  are discussed in Section 2.4.

### 2.3 Numerical Algorithm used in the SDS2 NOP Dynamic Compensator

The SDS2 NOP numerical compensator's algorithm employs 1st order backward finite difference method and is of the form

$$\begin{aligned} C_{alg_j}(t_k) &= C_{alg_j}(t_k - \Delta t_j) + \frac{\Delta t_j}{\tau_j + \Delta t_j} \cdot [A_j \cdot Dt(t_k) - C_{alg_j}(t_k - \Delta t_j)], \quad j = 1, \dots, 4; \\ SC_{alg}(t_k) &= \sum_{j=1}^4 C_{alg_j}(t_k) ; & \dots\dots\dots (5) \\ DtCmp_{alg}(t_k) &= (1 + \sum_{j=1}^4 A_j) \cdot Dt(t_k) - SC_{alg}(t_k) ; \end{aligned}$$

where:  $k = 1, 2, \dots$ ;  $i = 1, 2, \dots, 17$ ;

$C_{alg_{ij}}(t_0) = C_{ij}^0 = \text{initial conditions ; } t_0 = 0$  ;

The algorithm is resident in Darlington SDS2 trip computers. The individual discrete dynamic compensating terms  $C_{alg_{ij}}(t)$  (corresponding to the  $C_j(t)$  terms in the differential model.(4)) are periodically sampled with sampling times correspondingly equal to

$$\Delta t_1 = 3 \text{ sec, } \Delta t_2 = 30 \text{ sec, } \Delta t_3 = 300 \text{ sec, } \Delta t_4 = 3000 \text{ sec.}$$

The compensator algorithm (5) is described in the SDS2 Trip Computer Design Description (TCDD) document (Ref.4), its derivation is given in the Appendix A.

**2.4 Analytical Solutions to Compensator Differential Model**

Two different types of neutronic power  $\Theta_{NP}(t)$  variations are considered: a step-type change and a bounded ramp-type change. For each type of  $\Theta_{NP}(t)$  change the analytical, continuous-time solution to the compensator differential model (4) is given below.

Solution to Step-type Changes in Neutronic Power

Following assumption (A3), at the beginning of the analyzed transient ( $t_0 = 0$ ), the reactor is assumed to be at steady state at power  $b_0$ . The postulated step-type change in neutronic power  $\Theta_{NP}(t)$  is defined as

$$\Theta_{NP}(t) = \begin{cases} b & \text{for } t > 0; \\ b_0 & \text{for } t \leq 0; \end{cases} \dots\dots\dots (6)$$

where:  $b_0$  = initial reactor power level ;  
 $b$  = final reactor power level.

Solution of the linear differential model (4) with the step-type driving force is a standard problem (see e.g. Refs.8 and 9). Utilizing the assumptions (A1), (A3) and setting  $Dt(t) = \Theta_{NP}(t)$  with neutronic power step-type change  $\Theta_{NP}(t)$  specified by Eq.(6), the analytical solution to the differential compensator model (4) is

$$C_j(t) = C_j^0 \cdot e^{-\frac{t}{\tau_j}} + b \cdot A_j \cdot [1 - e^{-\frac{t}{\tau_j}}], \quad \text{with } C_j(0) = C_j^0 = A_j \cdot b_0 = \text{initial conditions};$$

$$j = 1, \dots, 4;$$

$$SC(t) = \sum_{j=1}^4 C_j(t);$$

$$DtCmp(t) = [1 + \sum_{j=1}^4 A_j] \cdot \Theta_{NP}(t) - SC(t); \dots\dots\dots (7)$$

$$t \geq 0$$

The initial conditions  $C_j(t=0) = C_j^0 = A_j b_0, j = 1, \dots, 4$ , imposed on the individual lag terms  $C_j(t)$  assure that the compensated detector  $DtCmp(t)$  at  $t = t_0$  reads exactly the steady state initial reactor power  $b_0$ , in agreement with the assumptions (A3) and (A4).

The case with **zero initial conditions** is important for the occasion when the SDS2 trip computer is "cold" restarted after the computer failure. In such a scenario we have to assume that the computer memory has been lost and therefore the computer has no available information regarding the last (recorded) reactor power. Hence, during the cold restart the "proper" initial conditions  $C_j^0 = A_j b_0, j = 1, \dots, 4$ , are not available and the only reasonable approach is to use the zero conditions  $C_j(0) = C_j^0 = 0, j = 1, \dots, 4$ . Accordingly, the sum  $SC(0) = 0$ , and the compensated detector response becomes

$$DtCmp(0) = (1 + \sum_{j=1}^4 A_j) \cdot \Theta_{NP}(0) - SC(0) = (1 + \sum_{j=1}^4 A_j) \cdot b_0 = 1.066 b_0;$$

It means, that the compensated detector response will initially exceed the initial reactor power by **6.6%** margin but such a bias is in the conservative direction.

### Solution to Bounded Ramp-type Changes in Neutronic Power

As before, we utilize assumption (A3), i.e. at the beginning of the analyzed transient ( $t_0 = 0$ ), the reactor is assumed to be at steady state power  $b$ . The bounded ramp-type change in neutronic power  $\Theta_{NP}(t)$  used in this analysis is defined as

$$\Theta_{NP}(t) = \begin{cases} (a \cdot t + b), & \text{for } 0 \leq t < t_1; \\ D, & \text{for } t \geq t_1; \end{cases} \dots \dots \dots (8)$$

where:  $b$  = initial reactor power level ,  
 $a$  = rate of power increase ,  
 $D$  = final reactor power level ,  
 $t_1$  = end time for the ramp driving force .

The time-solution to the compensator differential model (4) for bounded ramp-type variations in neutronic power is given by a combination of exponential functions. Utilizing assumptions (A1) and (A3), setting  $Dt(t) = \Theta_{NP}(t)$ , the **analytical solution** to the compensator differential model (4) for the bounded ramp-type change (8) in neutronic power  $\Theta_{NP}(t)$  is of the form

$$C_j(t) = \begin{cases} A_j \cdot (b + a \cdot [t - \tau_j \cdot (1 - e^{-\frac{t}{\tau_j}})]) - [A_j \cdot b - C_j^0] \cdot e^{-\frac{t}{\tau_j}}, & \text{for } 0 \leq t < t_1; \\ A_j \cdot D - [A_j \cdot D - C_j(t_1)] \cdot e^{-\frac{(t-t_1)}{\tau_j}}, & \text{for } t \geq t_1; \end{cases}$$

$$C_j(0) = C_j^0 = A_j \cdot b = \text{initial conditions ;}$$

$$j = 1, \dots, 4;$$

$$SC(t) = \sum_{j=1}^4 C_j(t) ;$$

$$DtCmp(t) = [1 + \sum_{j=1}^4 A_j] \cdot \Theta_{NP}(t) - SC(t) ; \dots \dots \dots (9)$$

$t \geq 0$

Mathematical derivation of the analytical solution (9) is given in the Appendix B.

As before, the initial conditions  $C_j(t=0) = C_j^0 = A_j b$ ,  $j = 1, \dots, 4$ , imposed on the ag terms  $C_j(t)$  assure that the compensated detector  $DtCmp(t)$  at  $t = 0$  reads exactly the steady state initial reactor power  $b$ , in agreement with the assumptions (A3) and (A4).

Discussion of the solution : An examination of the solution (9) indicates that boundary conditions and asymptotical trends of the solution are satisfied. In particular, observe the following properties of the solution:

(a) At  $t = 0$  the exponential terms  $e^{-\frac{t}{\tau_j}}$  equal to one, the term  $a \cdot [t - \tau_j \cdot (1 - e^{-\frac{t}{\tau_j}})]$  becomes zero, the two remaining terms  $A_j \cdot b$  cancel and the dynamic compensating terms  $C_j$  become equal to their initial conditions  $C_j(t=0) = C_j^0$ ,  $j = 1, \dots, 4$ , as they should. This property holds for any initial conditions  $C_j^0$ . Setting the initial conditions to  $C_j^0 = A_j b$ ,  $j = 1, \dots, 4$ ; as is the case with normal, uninterrupted

operation of the trip computers, the sum of  $C_j(t)$  terms becomes  $SC(t=0) = \sum_{j=1}^4 A_j \cdot b$ . At  $t = 0$  the reactor remains at its initial steady state  $b$ , hence the neutronic power is set to  $\Theta_{NP}(t=0) = b$ , and the terms  $\Theta_{NP}(0) \cdot \sum_{j=1}^4 A_j \cdot b$  and  $SC(t=0)$  in the expression for  $DtCmp(t)$  cancel. Hence, the compensated detector response becomes  $DtCmp(t=0) = \Theta_{NP}(t=0) = b$ . It means that at the initial steady state the compensated detector reads exactly the steady state neutronic power, i.e. no compensation is required, as we expect.

With the initial conditions  $C_j^0 = A_j \cdot b$ , the term  $[A_j \cdot b - C_j^0] = 0$ . In this case the rate of  $C_j(t)$  increase (or decrease, depending on the sign of rate  $a$ ) is, as shown in the Appendix B, described by the relation

$$\frac{dC_j}{dt} = A_j \cdot a \cdot \left[ 1 - e^{-\frac{t}{\tau_j}} \right]. \text{ Observe that at } t = 0 \text{ the rate is } \frac{dC_j}{dt} = 0, \text{ as expected, see e.g. Ref.8.}$$

The rate of change in the compensated detector response  $DtCmp(t)$  is shown in the Appendix B to be

$\frac{d}{dt} (DtCmp) = a \cdot \left[ 1 + \sum_{j=1}^4 A_j \cdot e^{-\frac{t}{\tau_j}} \right]$ , which implies that the **initial rate** (at  $t = 0$ ) is **increased** by the amount of  $\sum_{j=1}^4 A_j = 0.066$ , i.e. by **6.6%**, when compared with the rate 'a' of the neutronic power transient

$\Theta_{NP}(t)$ . This effect of the initial rate increase is evident in the calculated bounded ramp-type transients showed in Section 3.

(b) For  $t \rightarrow \infty$ ,  $\Theta_{NP}(t) = D$ , see Eq.(8), and the terms  $C_j$  (described by the solution part pertinent for  $t > t_1$ ) converge to their new steady states,  $C_j(t) \rightarrow A_j D$ ,  $j = 1, \dots, 4$ , regardless of the initial

conditions  $C_j^0$ . In the limit, the sum of  $C_j(t)$ ,  $SC(t) \rightarrow D \cdot \sum_{j=1}^4 A_j$  and  $DtCmp(t) \rightarrow \Theta_{NP}(t \geq t_1) = D$ , i.e.

the compensated detector response approaches the new steady state reactor power  $D$ , as expected, and no further compensation action is required.

(c) Intermediate times  $t < t_1$ , with  $t$  large by comparison with the time constants  $\tau_j$ .

With the initial conditions  $C_j^0 = A_j \cdot b$ , for large time  $t$ , such that the exponential term  $\left[ 1 - e^{-\frac{t}{\tau_j}} \right]$

approaches one, the rate  $\frac{dC_j}{dt} = A_j \cdot a \cdot \left[ 1 - e^{-\frac{t}{\tau_j}} \right] \rightarrow A_j \cdot a$ ; i.e. the lag compensating terms  $C_j(t)$  ramp up

(for positive 'a') with increasing rate, asymptotically approaching  $A_j \cdot a$  (which is the power ramp rate multiplied by the lag's gain coefficient). However, the  $C_j(t)$  transient is delayed in time with reference to the driving  $\Theta_{NP}(t)$  ramp, with the delay approaching time constant  $\tau_j$ , as it should be (see e.g. Ref.8 and 9).

For a ramp-type reduction in neutronic power  $\Theta_{NP}(t)$ , the ramp rate  $A_j \cdot a$  is negative and the situation is reversed, but the outcoming transient is delayed as before, with the delay approaching time constant  $\tau_j$ . For large  $t$ , but still before the point  $t_1$  of power saturation, the sum of exponential components

$\sum_{j=1}^4 A_j \cdot e^{-\frac{t}{\tau_j}}$  decreases and the rate  $\frac{d}{dt} (DtCmp)$  approaches the driving rate 'a'. This effect is caused by

dynamic action of the lagging term  $SC(t)$  acting towards a gradual reduction in rate magnitude, but its effect on the compensated detector rate is less visible (during the limited time span  $0 \leq t < t_1$ ), due to large time constants  $\tau_3$  and  $\tau_4$ .

The compensated detector responses  $DtCmp(t)$  described by Eqs.(7) and (9) are the exact mathematical solutions to the detector compensator model (3) and (4) for the postulated step-type and bounded ramp-type changes in neutronic power  $\Theta_{NP}(t)$ . Therefore, they serve as a reference against which the

compensated detector responses  $DtCmp\_alg(t_k)$  calculated by the numerical algorithm (5) are compared with.

## 2.5 Methodology and Objective of the Analysis

As mentioned before, the SDS2 NOP detectors signal are dynamically compensated. The dynamic compensation is realized digitally in the SDS2 trip computer software, utilizing the numerical compensation algorithm (5). Because of the finite difference form of the algorithm (5) and the four different sampling times  $\Delta t_j, j = 1, \dots, 4$  used in it, the resulting numerical compensation is computed with some error, relative to the "ideal" analytical compensator solution described by Eqs.(7) and (9).

The error  $\epsilon(t)$  of the compensator algorithm is defined (for a generic detector) as the difference between the reference compensated response  $DtCmp(t)$  given by the analytical solution (7) or (9), and the numerically compensated detector response  $DtCmp\_alg(t)$ . The numerical response  $DtCmp\_alg$  is calculated at discrete sampling times  $t = t_k$  by the numerical algorithm (5) as  $DtCmp\_alg(t_k)$ . Between the sampling times the numerically compensated response remains constant, namely

$$DtCmp\_alg(t) = DtCmp\_alg(t_k), \text{ for } t_k \leq t < t_{k+1}; \dots \dots \dots (10)$$

$$k = 0, 1, 2, \dots$$

Accordingly, the error of the numerical compensator algorithm is defined as

$$\epsilon(t) \triangleq DtCmp(t) - DtCmp\_alg(t), \quad t \in [0, T]; \dots \dots \dots (11)$$

The numerical error of the SDS2 compensator algorithm is broken into short and long terms, namely:

- **Short term error**  $STE(t)$ , defined as the compensator error  $\epsilon(t)$ , calculated over the first 300 sec of the transient, i.e.  $STE(t) = \epsilon(t), 0 \leq t \leq 300 \text{ sec};$   
(and)
- **Long term error**  $LTE(t)$ , defined as the compensator error  $\epsilon(t)$  calculated over times equal to or greater than 300 sec, i.e.  $LTE(t) = \epsilon(t), t > 300 \text{ sec}.$

### Timing Effect of the Dynamic Compensating Term's Simultaneous Actions

The timers of the four dynamic compensating terms  $C\_alg_j(t_k), j = 1, \dots, 4$  trigger their individual compensating actions correspondingly at sampling times  $\Delta t_j, j = 1, \dots, 4$ . Because the timers are synchronized, every 3000 sec the four compensating terms  $C\_alg_j$  are triggered simultaneously. The moment  $t_{act}$  of occurrence of the first simultaneous compensating action of the four terms, with respect to the initiation moment  $t_0$  of the neutronic power  $\Theta_{np}(t)$  change, considerably affects the magnitude and sign of compensator's error transient, particularly for the large, step-type changes in neutronic power. This effect was analysed by simulating the two extreme scenarios :

(1) The power change starts at moment  $t_0 = 0$ . Then, the four compensating terms are triggered sequentially, with the fastest term  $C\_alg_1$  triggered for the first time at the moment  $t_1 = t_0 + \Delta t_1 = 3 \text{ sec}$ , the second term  $C\_alg_2$  triggered for the first time at  $t_2 = t_0 + \Delta t_2 = 30 \text{ sec}$ ,  $\dots$ , and the slowest term  $C\_alg_4$  triggered for the first time at  $t_4 = t_0 + \Delta t_4 = 3000 \text{ sec}$  (at time  $t_4$  the four timers are triggered simultaneously). In this scenario the two slowest compensating terms  $C\_alg_3$  and  $C\_alg_4$  are brought into action for the first time at the latest possible times after power change initiation. As a result, the compensator error decreases at a slower rate over the transient duration.

(2) The power change starts at the moment  $t_0 = 0$ , but the four dynamic terms  $C\_alg_j, j = 1, \dots, 4$ ; are triggered (for the first time) to act simultaneously, immediately after the power transient initiation, namely at  $t_{act} = t_0 + \Delta t = 0.3 \text{ sec}$ , where  $\Delta t = 0.3 \text{ sec}$  is the fastest sampling time, used to calculate the points of the analytical solution (ten times shorter than the sampling time  $\Delta t_1$  of the fastest compensating term

$C_{alg_1}$ ). In this case the multiplicative coefficients  $\frac{\Delta t_j}{\tau_j + \Delta t_j}$ ,  $j = 1, \dots, 4$  in the numerical compensator algorithm (5) are initially, at  $t = t_{act}$ , much larger than they were designed to be for the backward finite difference algorithm, particularly for the slower compensating terms, with larger  $\Delta t_j$ . As a result, the numerical compensator initially significantly "overcompensates" the detector response. The sign of the resulting error is reversed when compared with the error in the identical case analyzed under the scenario (1) and the initial magnitude of the error is larger. Also, the error transient decreases faster with time than in the first scenario. In the next successive discrete moments, just after  $t_{act}$  the algorithm returns to the sequential mode of operation, and for the remaining part of the transient the proper values of the multiplicative coefficients are used.

The time  $t_{act}$  of that first simultaneous compensating action by the four dynamic terms varies randomly with respect to the initiation moment  $t_0$ . Therefore, the action timing difference  $\eta_{act} = (t_{act} - t_0)$  which describes the relative timing of the first simultaneous compensating action, is a **random variable**. The variable  $\eta_{act}$  is bounded, i.e. for the SDS2 numerical compensator  $0 \leq \eta_{act} \leq 3000$  sec and therefore is described by a truncated probability distribution. It follows that, depending on the actual value of the variable  $\eta_{act}$ , the magnitude of the resulting compensator error  $\epsilon(t)$  varies randomly but is also bounded in magnitude.

**Objective of the Analysis :** The objective of the analysis is to simulate the error transients  $\epsilon(t)$  of the detector compensation algorithm (5), for a specified family of neutronic power transients. Then, analyze the calculated error transients and evaluate their maximum short and long term errors  $\max [STE(t)]$  and  $\max [LTE(t)]$ , while taking into account the timing effects of the simultaneous correcting actions of the compensating lag terms  $C_{alg_j}$ .

A simulation code **DACER** (Detector Algorithmic Compensation Error) was used in the calculations. It has been specifically developed for the purpose of analysis of SDS2-NOP numerical compensation and utilizes MATLAB software (see Ref.12). The code emulates the digital compensator algorithm (5) to yield the numerically compensated generic detector response  $DtCmp_{alg}(t)$ . The analytical solutions (7) and (9) are used for the calculation of the compensated detector "ideal" response  $DtCmp(t)$  for the specified family of neutronic power transients  $\Theta_{NP}(t)$ . The code then calculates the compensator's error transients  $\epsilon(t)$  as defined by Eq.(11). It also enables to directly evaluate the timing effects of the simultaneous correcting actions by the compensating dynamic terms  $C_{alg_j}(t)$ .

The potential effect of the SDS2 NOP trip logic on the numerical compensator error is beyond the scope of this analysis. List of neutronic power transients used for the detailed error analysis is given in the next section.

### 3. Computational Results

The family of neutronic power transients  $\Theta_{NP}(t)$  specifically requested and agreed upon with Darlington ND Nuclear Safety Department for detailed error analysis, consequently simulated by the DACER code and analysed, is given below :

- (a) ramp-type power increase from 0% to 126% FP in one hour;
- (b) ramp-type power increase from 0% to 126% FP in 12 hours;
- (c) ramp-type power reduction from 100% FP to 60% FP in 0.5 hour;
- (c-bis) ramp-type neutronic power reduction from 100% FP to 60% FP in 0.5 hour with zero initial conditions in dynamic compensating terms;
- (d) ramp-type power reduction from 100% FP to 60% FP in 6 hours;

- (e) ramp-type power increase from 0% to 126% FP in one hour, with the four compensator timers set to trigger their first compensating action simultaneously, just after the power ramp initiation;
- (f) step-type power increase from 0% to 126% FP;
- (g) step-type power increase from 0% to 126% FP, with the four compensator timers set to trigger their first compensating action simultaneously, just after the power step initiation;
- (h) step-type power reduction from 100% FP to 60% FP.
- (i) step-type power reduction from 100% FP to 60% FP, with the four compensator timers set to trigger their first compensating action simultaneously, just after the initiation of the power step reduction.

The Cases (a),(b),(c),(c-bis),(d),(f) and (h) were simulated assuming the sequential mode of operation. The remaining Cases (e),(g) and (i) were simulated with the four dynamic terms  $C_{alg_j}(t)$  initiating their first simultaneous compensating actions immediately after the power step initiation. Simulation results for the Cases (a),(b),(f) and (g) are briefly described below, in Sections 3.1, 3.2 and 3.3. Detailed description and analysis of the simulation results for all the listed cases is given in Ref.5.

### 3.1 Bounded Ramp-type Changes in Neutronic Power

#### Case (a): Ramp-type Neutronic Power Increase from 0% FP to 126 %FP in One Hour.

The parameters of the bounded  $\Theta_{NP}(t)$  ramp in Case (a) are:

$$\begin{aligned}
 t_0 &= 0 = \text{ramp initial time ;} & t_1 &= 3600 \text{ sec} = \text{ramp end ( cut-off ) time ;} \\
 b &= 0 \text{ FP} = \text{initial power level ;} & D &= 1.26 \text{ FP} = \text{final (bounding) power level ;} \\
 a &= 1.26 \text{ FP/hr} = 3.50 \times 10^{-4} \text{ FP/sec} = \text{ramp rate ;} \\
 T &= 10,000 \text{ sec} = \text{duration of the simulation transient .}
 \end{aligned}$$

Results of the simulation are presented in Figs. 2, 3, 4 and 5. The dashed lines in Fig.2 represent the postulated bounded ramp-type change in neutronic power  $\Theta_{NP}(t)$ , calculated following the relation (8). The analytical response  $DtCmp(t)$  of the compensated generic detector, calculated following the analytical solution (9) is shown in the upper-half of Fig.2, marked by the solid line. In the lower-half of Fig.2 the numerically compensated detector response  $DtCmp_{alg}(t)$ , calculated by the numerical compensation algorithm (5) is shown in the solid line. The transients in the upper and lower halves of Fig.2 look the same, which implies that the numerical compensation algorithm (5) provides good representation of the "ideal" analytical solution (9).

The transient of the compensator's numerical algorithm error  $\epsilon(t)$ , defined by relation (11) as a difference between  $DtCmp(t)$  and  $DtCmp_{alg}(t)$  is depicted in Fig.3 using a magnified scale, in fraction of %FP. For most of the transient the calculated numerical error  $\epsilon(t)$  is negative. It implies, that for cases with power increase the generic detector signal compensated by the numerical algorithm (5) is larger than its equivalent "ideal" analytical compensation solution, and therefore is conservative. During the whole transient the error  $\epsilon(t)$  remains within the allowable long-term tolerance envelope of  $\pm 0.25$  %FP. At 3600 sec, which is actually the cut-off time of the power ramp, the error reaches its largest (negative) value of  $-0.2$  %FP. After that the error oscillations decrease exponentially.

Transients of the individual dynamic compensating terms  $C_{alg_j}(t)$ ,  $j=1, \dots, 4$ , and their corresponding sum  $SC_{alg}(t)$ , calculated by the numerical compensation algorithm (5) are shown correspondingly in the upper and lower-halves of Fig.4. They are sampled periodically at times  $t_k$ ,  $k = 0, 1, 2, \dots$  and remain constant between the sampling times. For comparison, the "ideal" transients of the continuous dynamic compensating terms  $C_j(t)$ ,  $j=1, \dots, 4$  and their sum  $SC(t)$ , calculated using the analytical solution (9) are shown in Fig.5.

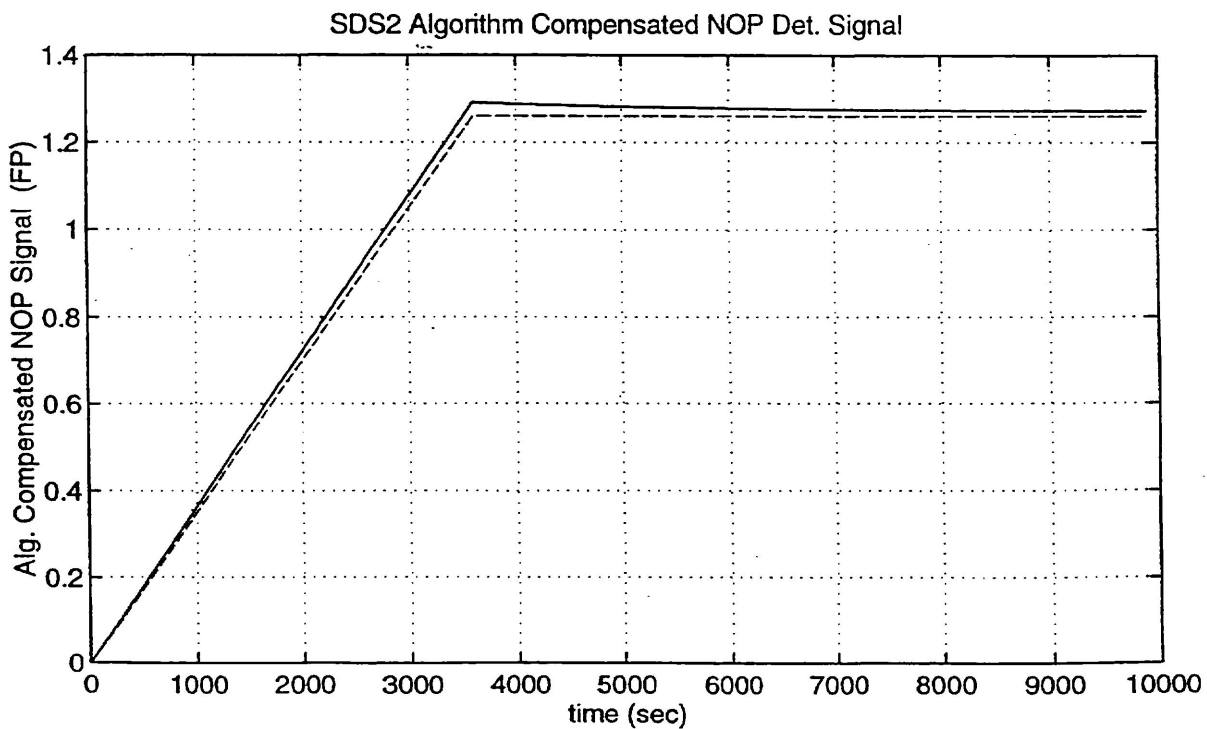
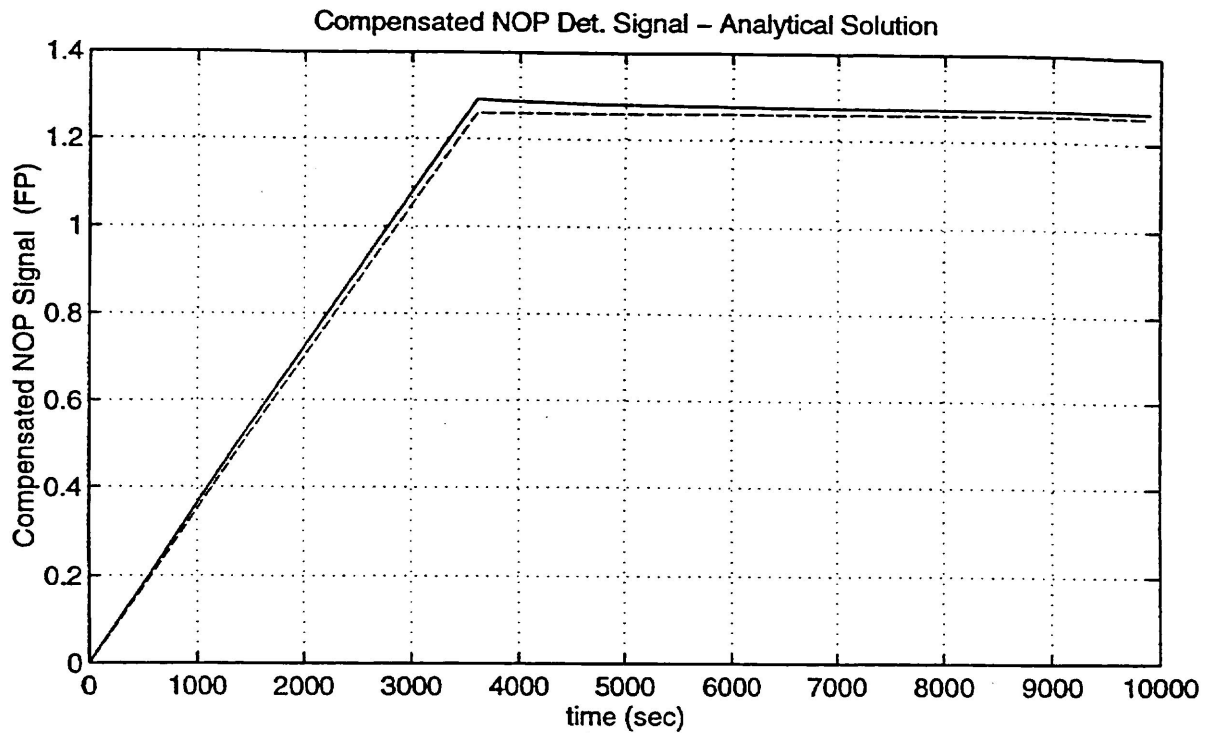


Figure 2 . Bounded Ramp from 0 %FP to 126 %FP in 1 hours.

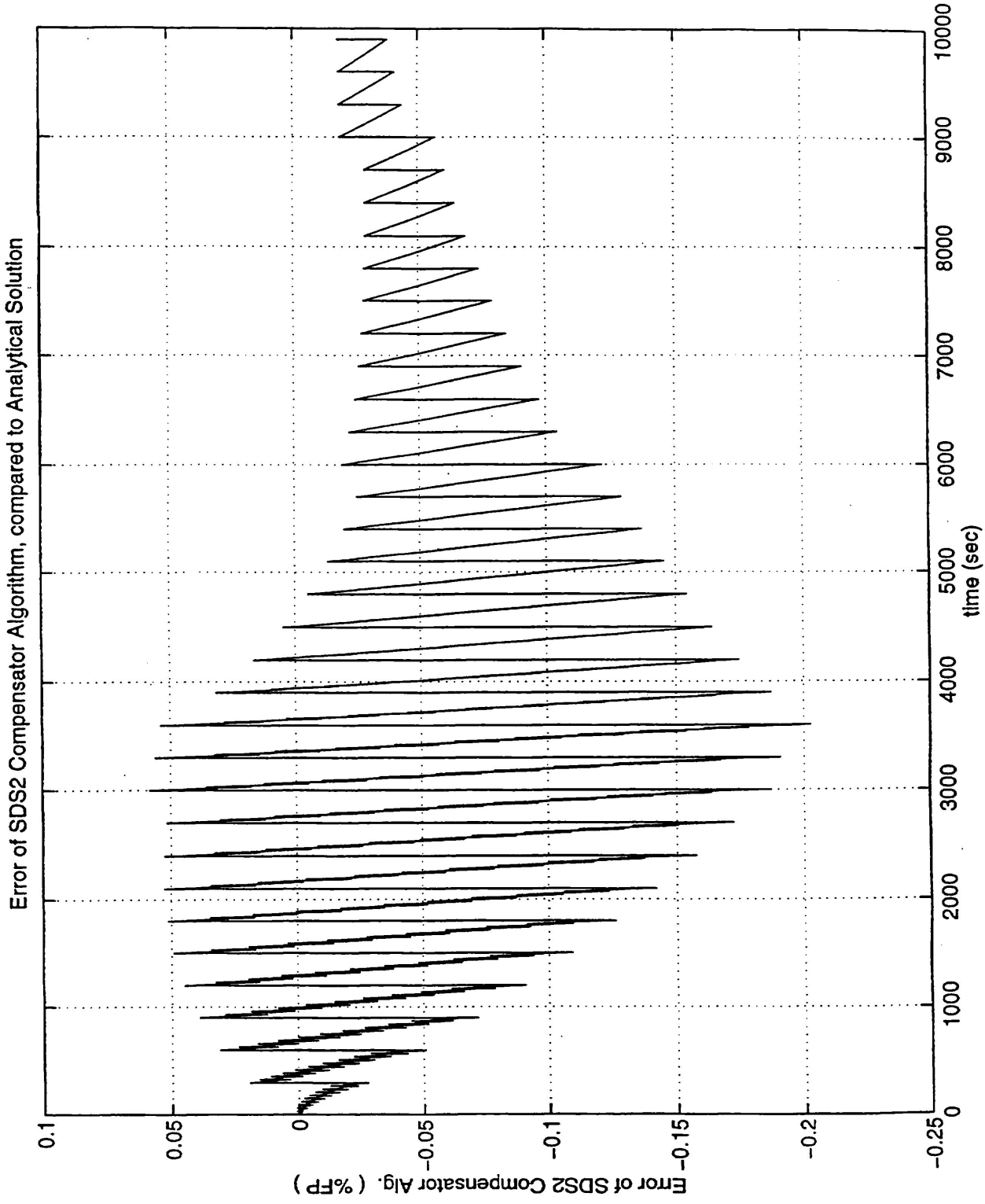


Figure 3. Bounded Ramp from 0 %FP to 126 %FP in 1 hours.

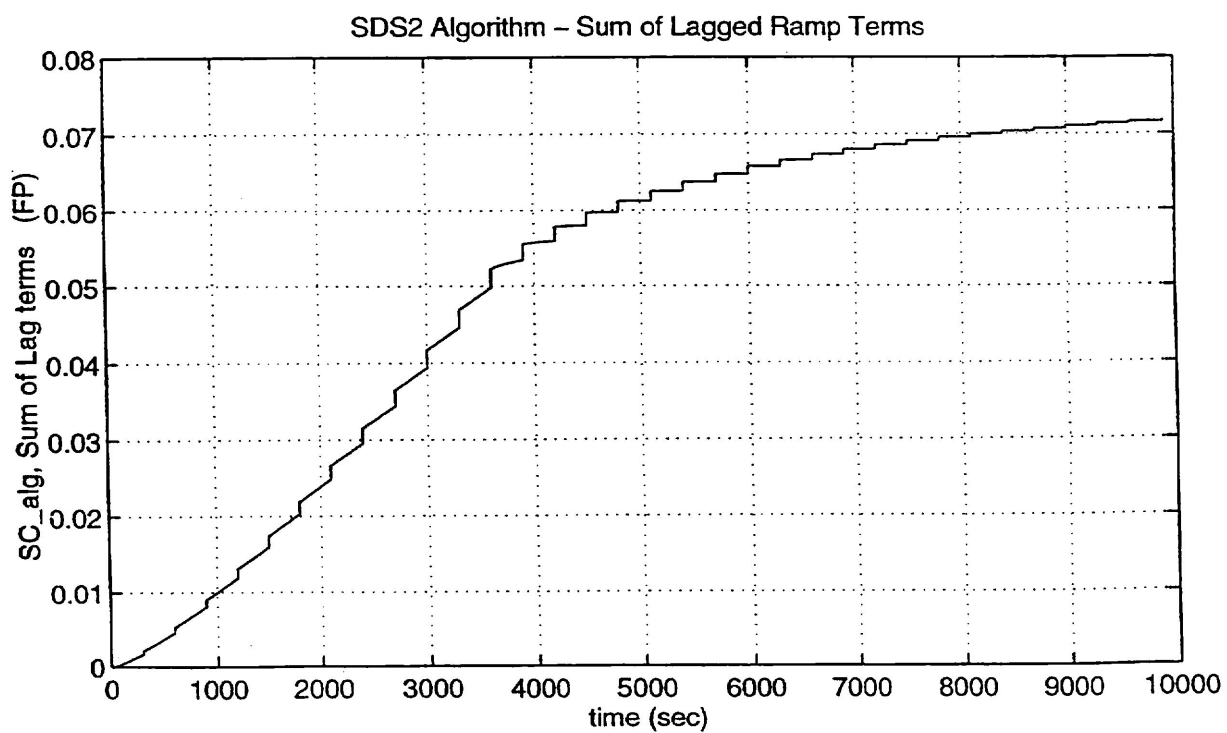
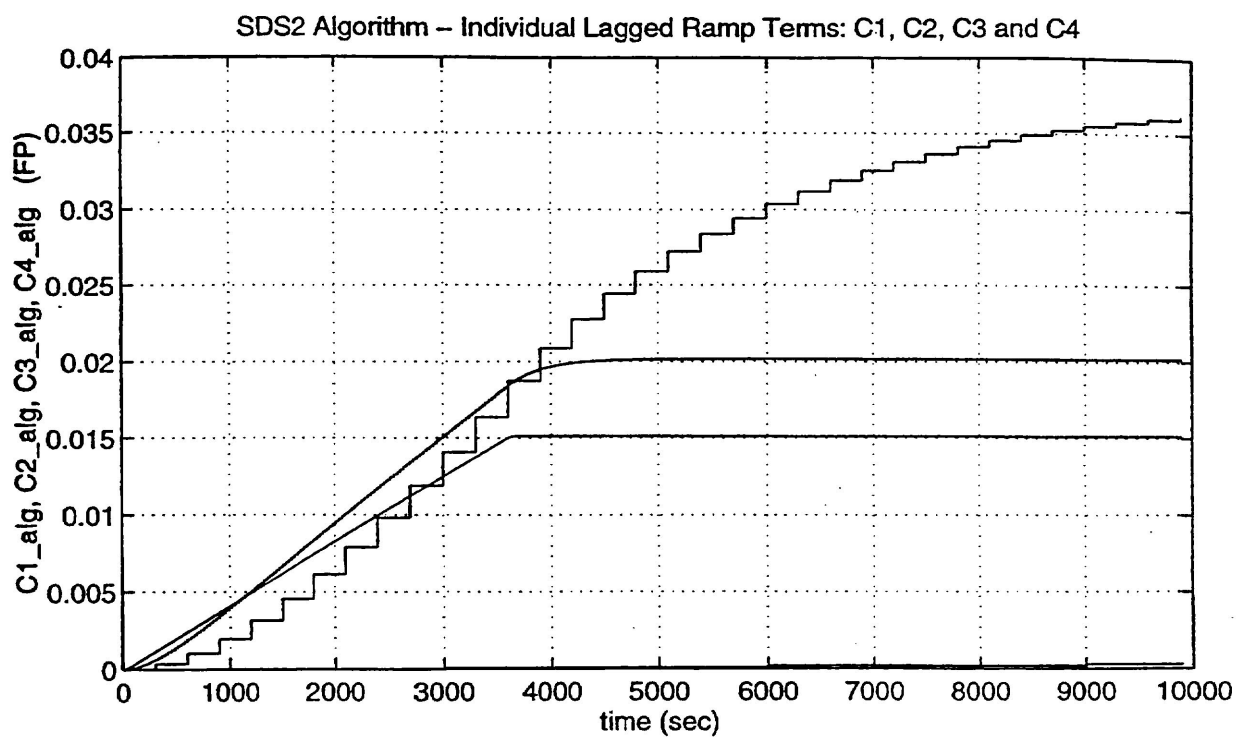


Figure 4. Bounded Ramp from 0 %FP to 126 %FP in 1 hours.

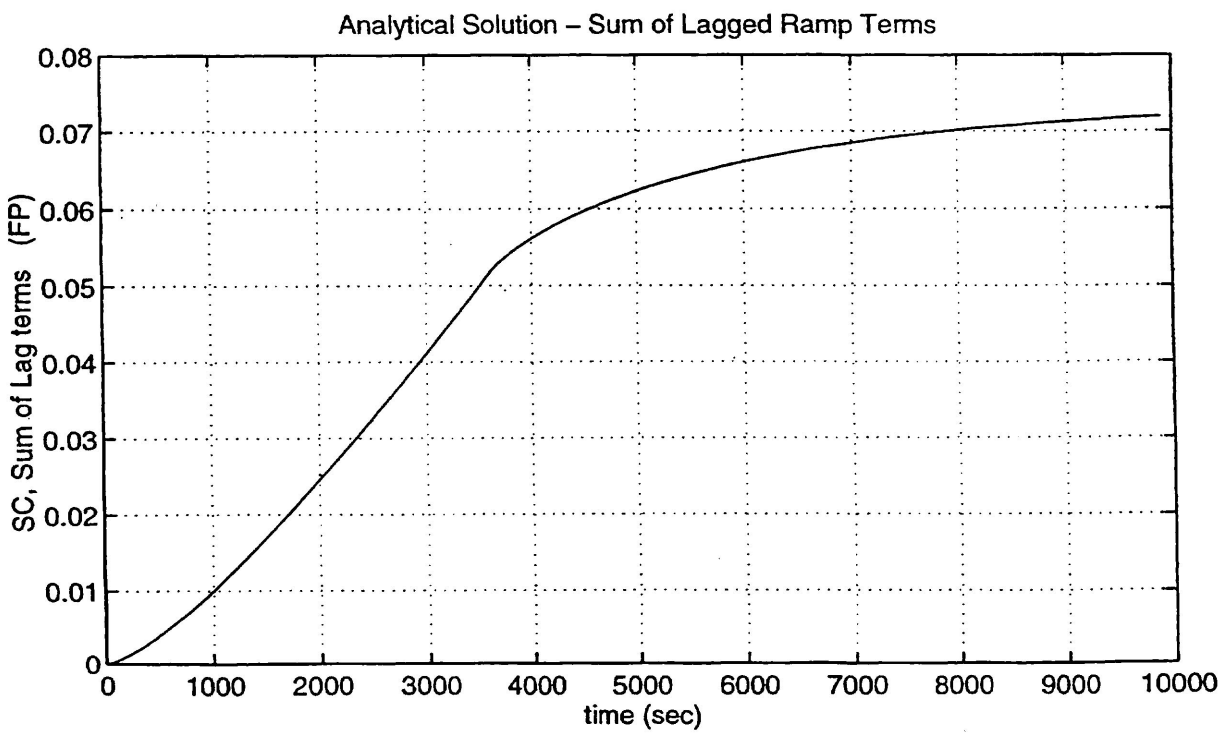
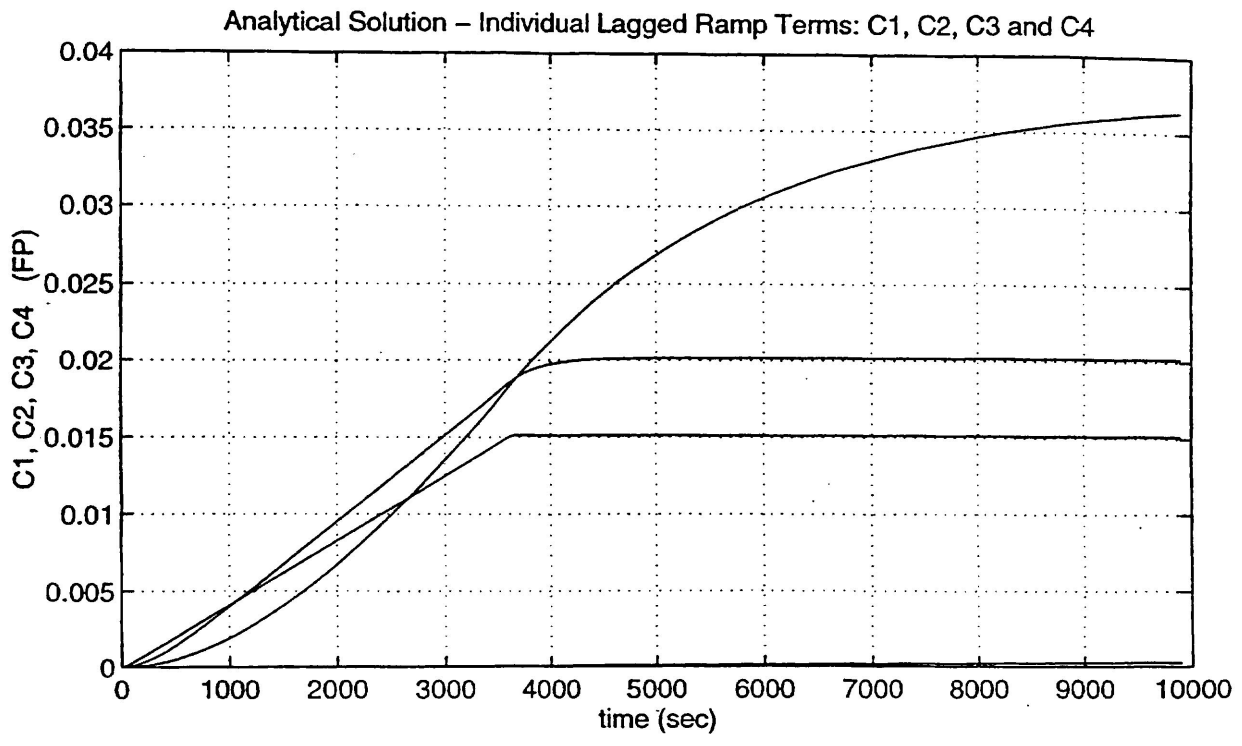


Figure 5. Bounded Ramp from 0 %FP to 126 %FP in 1 hours.

Between the (large) sampling moments  $t_n = 300\text{ s}, 600\text{ s}, 900\text{ s}, \dots$ , the error  $\epsilon(t)$  is growing in almost ramp-type fashion (in negative direction), due to the continuous increase of the analytically calculated compensated response  $DtCmp(t)$ . At each sampling moment  $t_n$  the error is momentarily reduced to a small value by the correcting action of the numerically calculated third compensating term  $C_{alg_3}$ . As a result, the error transient depicted in Fig.3 shows a series of spikes with increasing amplitudes (up to the ramp cut-off time  $t_1 = 3600\text{ sec}$ ). The spikes occur periodically every 300 sec, which is the sampling time  $\Delta t_3$  of the third dynamic compensating term  $C_{alg_3}$ . Because the gain coefficient  $A_3 = 0.03$  of that term amounts to almost half of  $\sum_{j=1}^4 A_j = 0.066$ , the effect of the corrections introduced by the third compensating term is much larger than the corrections introduced by the fast first two terms  $C_{alg_1}$  and  $C_{alg_2}$ . Also, due to its large time constant  $\tau_3 = 2400\text{ sec}$  and the large sampling time  $\Delta t_3 = 300\text{ sec}$ , the compensating action of the third term spreads over the long time duration. As a result, the **third** numerical dynamic term  $C_{alg_3}(t_k)$  is the **dominant contributor** to the error  $\epsilon(t)$ .

The first two dynamic terms  $C_{alg_1}$  and  $C_{alg_2}$  affect the overall error transient in a similar fashion, but less significantly. The effect of the fourth compensating term  $C_{alg_4}$  is barely noticeable within the 10,000 second transient duration time, because of its huge time constant of  $\tau_4 = 300,000\text{ sec}$ , very large sampling time  $\Delta t_4 = 3000\text{ sec}$  and the smallest gain coefficient  $A_4 = 0.008$ . The influence of this term can be observed only very far into the transient, near the steady state.

To better illustrate the contributing effect of the two fastest dynamic compensating terms  $C_{alg_1}$  and  $C_{alg_2}$ , the first 350 seconds of the compensator error  $\epsilon(t)$  transient is shown separately in Fig.6, in a magnified scale. The individual action of the first dynamic term  $C_{alg_1}$  is manifested by the small,

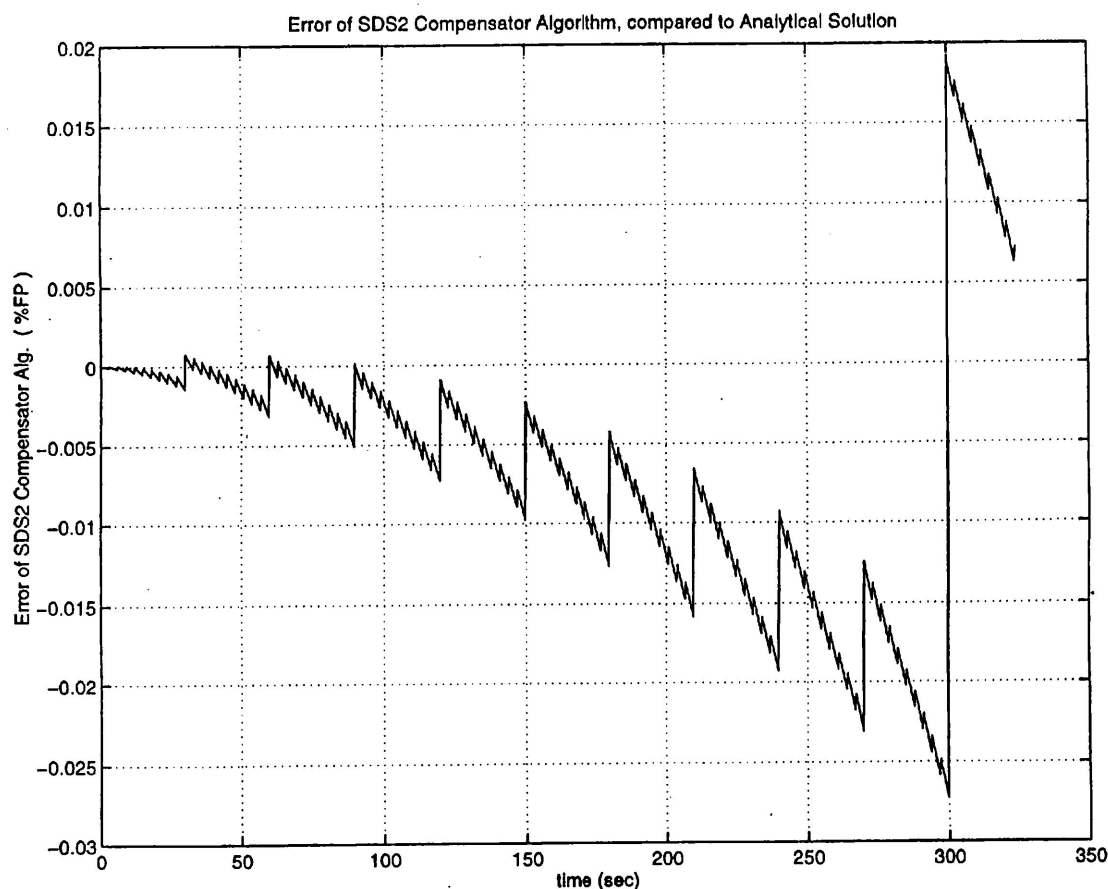


Figure 6. Bounded Ramp from 0 %FP to 126 %FP in 1 hours.

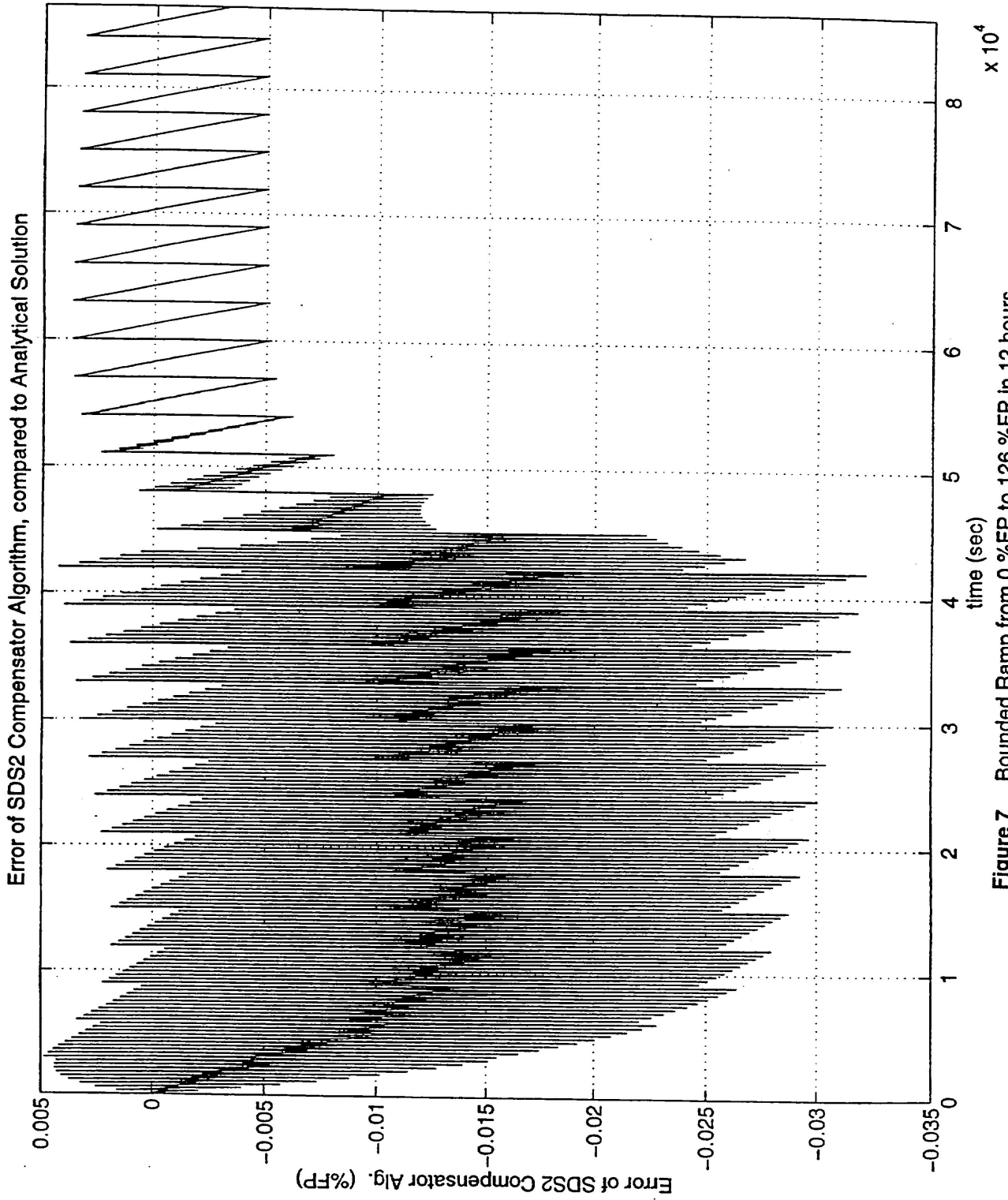


Figure 7. Bounded Ramp from 0 %FP to 126 %FP in 12 hours.

periodical "seesaw-type" line with  $\Delta t_1 = 3$  sec sampling time. It is superimposed on the larger seesaw-type transient with  $\Delta t_2 = 30$  sec sampling time, which represents the impact of the second dynamic compensating term  $C_{alg_2}$ . The seesaw-type oscillatory behavior is caused by the fact that the compensation error  $\epsilon(t)$  is calculated as a difference between the continuously changing analytical sum  $SC(t)$  and the periodically sampled numerical term  $SC_{alg}(t)$ . At 300 sec time the third dynamic term  $C_{alg_3}$  comes into action and, as described before, its effect is dominant by comparison with the impact of the first two terms.

### Case (b): Ramp-type Neutronic Power Increase from 0%FP to 126 %FP in 12 Hours.

The parameters of the bounded  $\Theta_{NP}(t)$  ramp in Case (b) are:

$$\begin{aligned} t_0 &= 0 = \text{ramp initial time ;} & t_1 &= 12 \text{ hrs} = \text{ramp end (cut-off) time ;} \\ b &= 0 \text{ FP} = \text{initial power level ;} & D &= 1.26 \text{ FP} = \text{final (bounding) power level ;} \\ a &= 0.105 \text{ FP/hr} = 2.917 \times 10^{-5} \text{ FP/sec} = \text{ramp rate ;} \\ T &= 24 \text{ hrs} = \text{duration of the simulation transient.} \end{aligned}$$

This is a much slower transient than in Case (a). For brief, only the compensator numerical algorithm's error  $\epsilon(t)$  is plotted in Fig.7 above, in fraction of %FP, using a magnified scale. Up to the cut-off power ramp time  $t_1 = 12$  hrs the calculated error  $\epsilon(t)$  is negative, which implies (as before) that for cases with power increase the numerically compensated detector signal is larger than its corresponding "ideal" analytical solution, and hence is conservative. For time  $t > t_1$  the error diminishes and oscillates about 0 %FP, with a very small amplitude and a period of 3000 sec, equal to the sampling time  $\Delta t_4$  of the slowest dynamic compensating term  $C_{alg_4}$  with the time constant of  $\tau_4 = 300,000$  sec. In a very long transient like this one, the 4<sup>th</sup> dynamic term has enough time to become effective and becomes a significant contributor to the compensator dynamical error  $\epsilon(t)$ .

The largest (in magnitude) compensation error is very small, of about  $-0.032$  %FP and occurs just before the power cut-off time  $t_1$ .

## 3.2 Step-type Changes in Neutronic Power

### Case (f): Step-type Increase in Neutronic Power from 0%FP to 126 %FP.

This is the most critical of the analyzed cases, because a very large, "instantaneous" jump in neutronic power, from 0 %FP to the SDS2 NOP trip setpoint is postulated.

The parameters of the step increase in neutronic power  $\Theta_{NP}(t)$  in Case (f) are:

$$\begin{aligned} t_0 &= 0 = \text{initial time ;} & T &= 5400 \text{ sec} = \text{duration of the simulation transient ;} \\ b_0 &= 0 \text{ FP} = \text{initial power level ;} & b &= 1.26 \text{ FP} = \text{final power level.} \end{aligned}$$

Main results simulation are presented in Figs. 8, 9 and 10. The "ideal" response of the compensated detector  $DtCmp(t)$ , calculated using the analytical representation (7), is shown in the upper-half of Fig.8, marked by a solid line. The numerically compensated detector response  $DtCmp_{alg}(t)$ , calculated using the numerical algorithm (5), is presented in the lower-half of Fig.8, plotted by a solid line. Dashed lines depict the postulated step-type increase in neutronic power  $\Theta_{NP}$ .

In this case the reactor is initially at steady state, at zero power level  $b_0 = 0$  FP. Accordingly, the initial conditions imposed on the dynamic compensating terms  $C_j$  and  $C_{alg_j}$  are equal to zero, i.e.

$$C_j(0) = C_j^0 = A_j \cdot b_0 = 0 \text{ FP ;} \quad \text{and} \quad C_{alg_j}(0) = C_j^0 = A_j \cdot b_0 = 0 \text{ FP ;} \quad (12)$$

$$j=1, \dots, 4 \qquad \qquad \qquad j=1, \dots, 4$$

as well as their corresponding sums  $SC\_alg(0) = 0 \text{ FP}$ ,  $SC(0) = 0 \text{ FP}$ . Hence, the initial compensated detector responses are also zero, since (see Eq.(7) and Eq.(5))

$$\begin{aligned} DtCmp(0) &= \left[1 + \sum_{j=1}^4 A_j\right] \cdot \Theta_{NP}(0) = \left[1 + \sum_{j=1}^4 A_j\right] \cdot b_0 = 0 \text{ FP}; \quad \text{and} \\ DtCmp\_alg(0) &= \left[1 + \sum_{j=1}^4 A_j\right] \cdot Dt(0) = \left[1 + \sum_{j=1}^4 A_j\right] \cdot b_0 = 0 \text{ FP}; \end{aligned} \quad (13)$$

Immediately after the power step increase, at  $t = 0^+$  the dynamic terms  $C_j$ ,  $C\_alg_j$ ,  $j = 1, \dots, 4$  and their sums  $SC$  and  $SC\_alg$  are still equal to zero, but the neutronic power and the uncompensated detector (ideal) reading momentarily increase to  $\Theta_{NP}(0^+) = b = 1.26 \text{ FP}$ ,  $Dt(0^+) = b = 1.26 \text{ FP}$ .

Accordingly, the compensated detector responses  $DtCmp$  and  $DtCmp\_alg$  jump to 1.34 FP level, because

$$DtCmp(0^+) = \left[1 + \sum_{j=1}^4 A_j\right] \cdot \Theta_{NP}(0^+) = \left[1 + \sum_{j=1}^4 A_j\right] \cdot b = (1 + 0.066) \cdot 1.26 \text{ FP} = 1.34 \text{ FP};$$

and

$$DtCmp\_alg(0^+) = \left[1 + \sum_{j=1}^4 A_j\right] \cdot Dt(0^+) = \left[1 + \sum_{j=1}^4 A_j\right] \cdot b = (1 + 0.066) \cdot 1.26 \text{ FP} = 1.34 \text{ FP};$$

This step-type jump is clearly visible in both parts of Fig.8. For  $t > 0^+$  the both responses exponentially approach the 1.26 FP level, which is the reactor new steady state.

The transient of the compensator's numerical algorithm error  $\epsilon(t)$  is depicted in Fig.9 as a fraction of %FP. For the whole transient the calculated error is strongly negative, from about  $-0.1 \text{ %FP}$  to below  $-0.5 \text{ %FP}$ , which implies that for rapid power increases the numerically compensated (by the trip computer) detector signal is conservative. The amplitudes of the error oscillations decrease exponentially. As in previous cases, the dominant influence of the third dynamic compensating term  $C\_alg_3$  with the time constant  $\tau_3 = 2400 \text{ sec}$  and the largest gain coefficient  $A_3 = 0.030$  is evident. The effect of the slowest dynamic term  $C_4$  (with the time constant  $\tau_4 = 300,000 \text{ sec}$  and the sampling time  $\Delta t_4 = 3000 \text{ sec}$ ) is impossible to observe in this relatively short simulation run.

Transients of the individual dynamic compensating terms  $C\_alg_j(t)$ ,  $j=1, \dots, 4$ , calculated using the numerical algorithm (5) are shown in the upper-half of Fig.10. Discretization in the transient of the second fastest term  $C\_alg_2$  with the time constant  $\tau_2 = 300 \text{ sec}$  and sampling time  $\Delta t_2 = 30 \text{ sec}$  is clearly visible, but the transient of the fastest term  $C\_alg_1$  (with  $\Delta t_1 = 3 \text{ sec}$  sampling) looks like a continuous line. The transient of the slowest term  $C\_alg_4$  can be hardly noticed. It occurs at 3000 sec time and has a form of a very small step, due to the fact that at that time a substantial part of the error has already been compensated by the faster terms.

Transient of the the sum  $SC\_alg(t)$  of the four dynamic terms  $C\_alg_j$ ,  $j=1, \dots, 4$ ; is depicted in the lower-half of the same figure.

For a better illustration of the error dynamics, the first 1000 sec of the error transient  $\epsilon(t)$  is shown in Fig.11. The effect of time discretization in the two fastest compensating terms  $C\_alg_1$  and  $C\_alg_2$ , with time constants  $\tau_1 = 30 \text{ sec}$  and  $\tau_2 = 300 \text{ sec}$  is emphasized.

The maximum (in magnitude) short term error (based on Fig.11) is  $\max [STE(t)] = -0.56 \text{ %FP}$  and occurs at 300 sec. The maximum long term error occurs at 600 sec and is  $\max [LTE(t)] = -0.47 \text{ %FP}$ . More detailed description of the case is given in Ref.5.

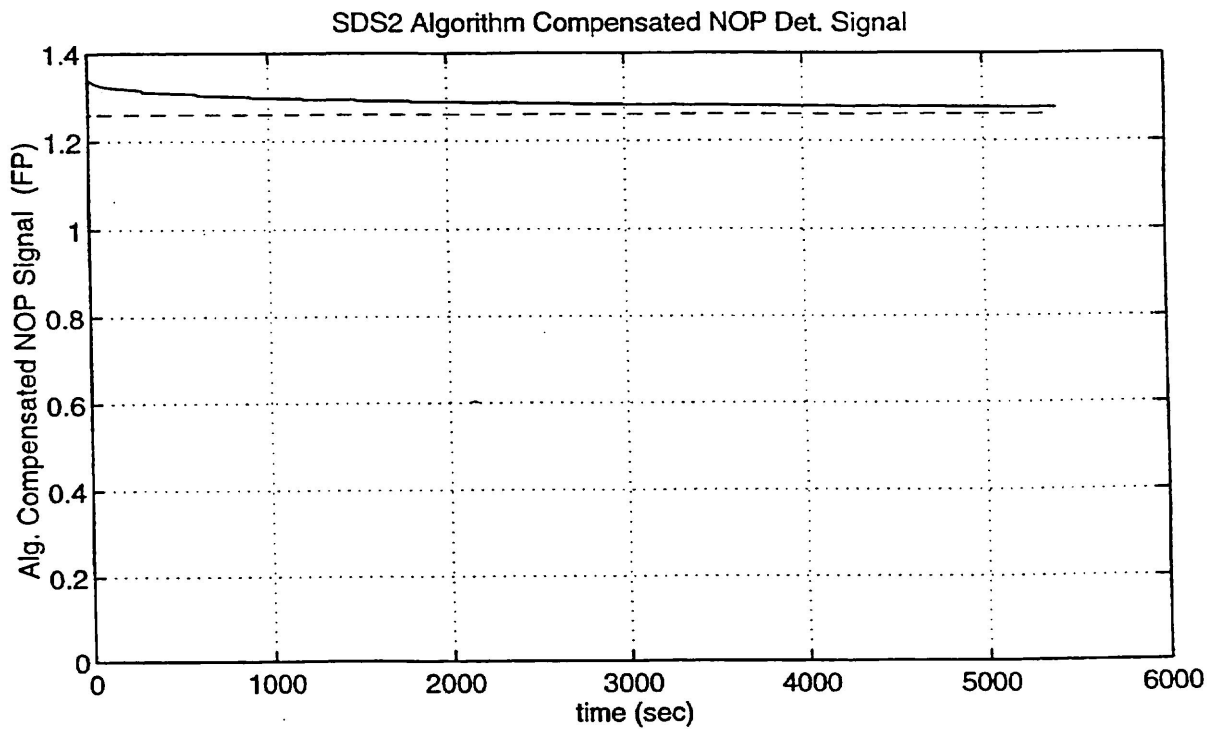
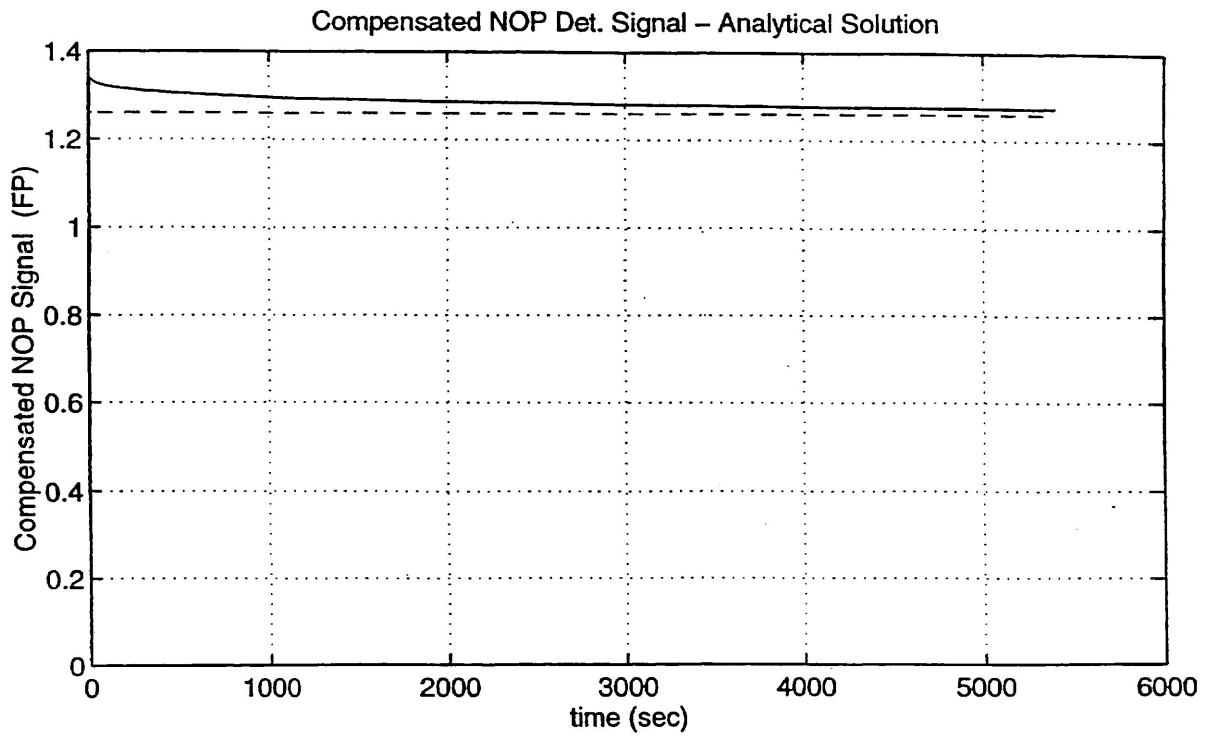


Figure 8. Power Step from 0 %FP to 126 %FP at  $t_0 = 0$

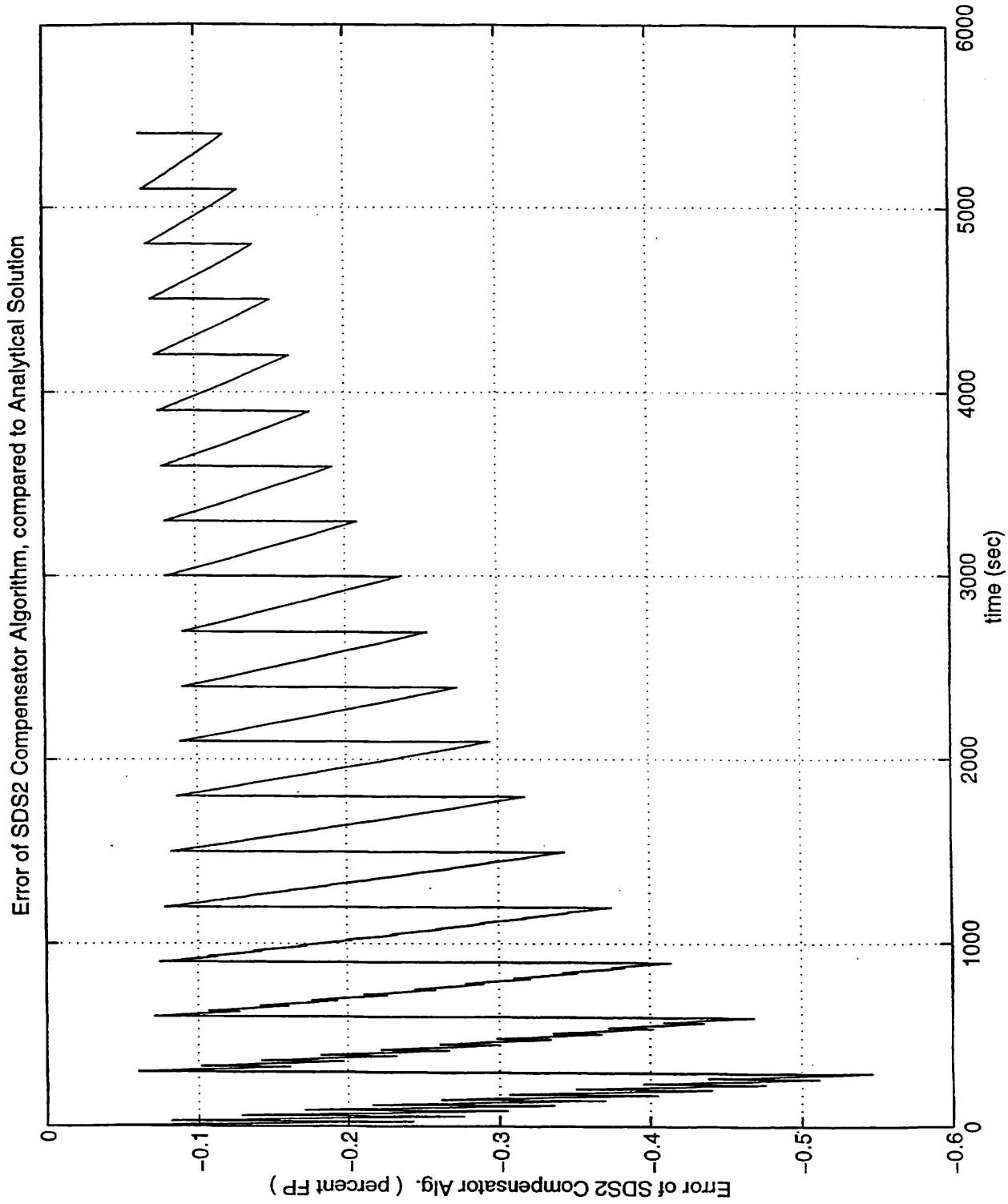


Figure 9. Power Step from 0 %FP to 126 %FP at t0 = 0

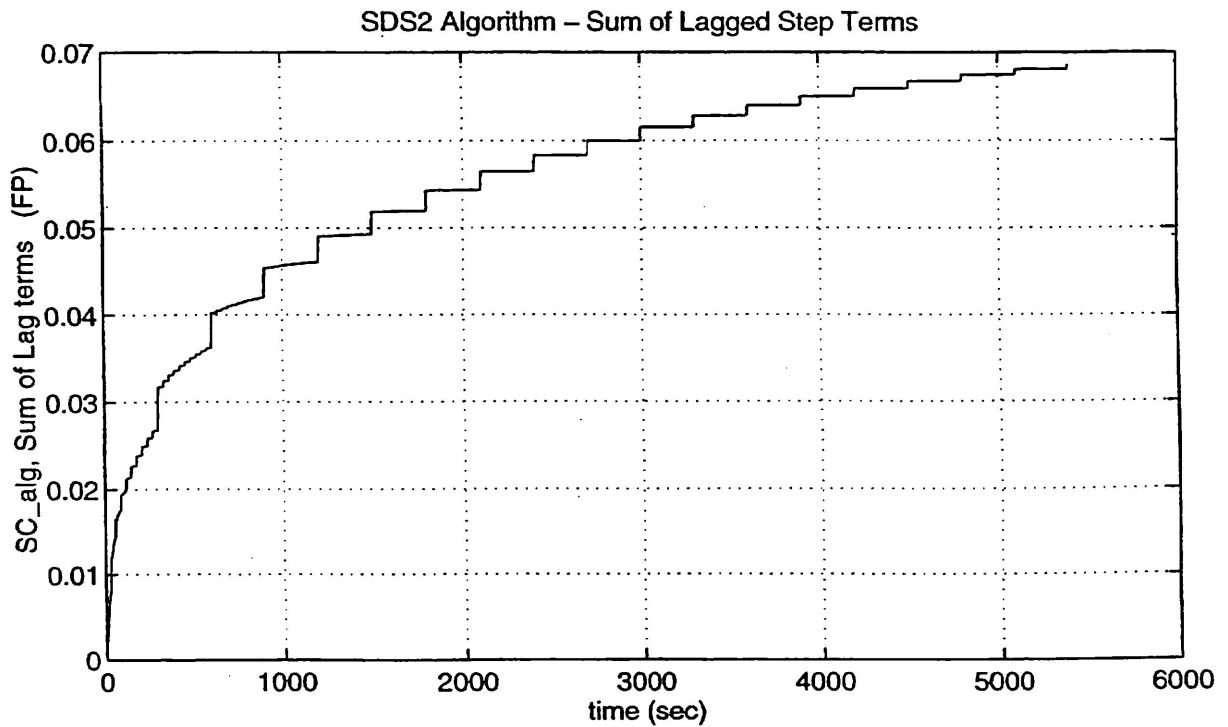
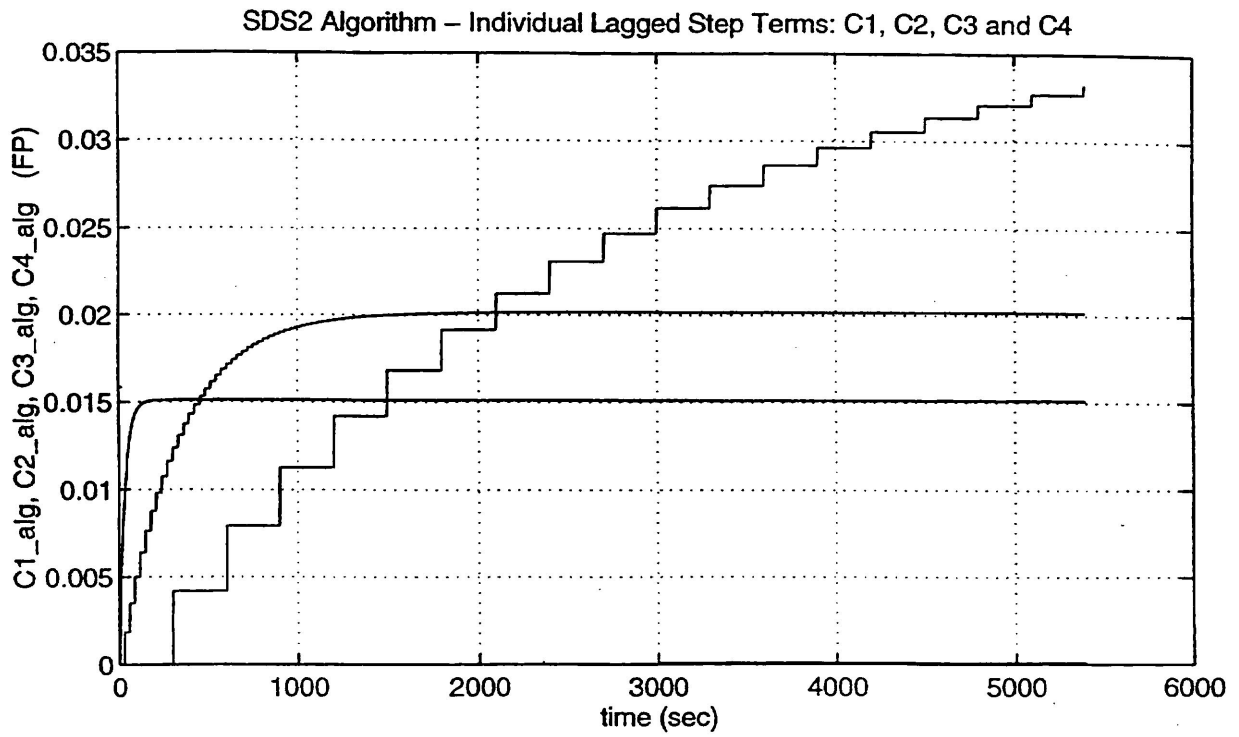


Figure 10. Power Step from 0 %FP to 126 %FP at  $t_0 = 0$

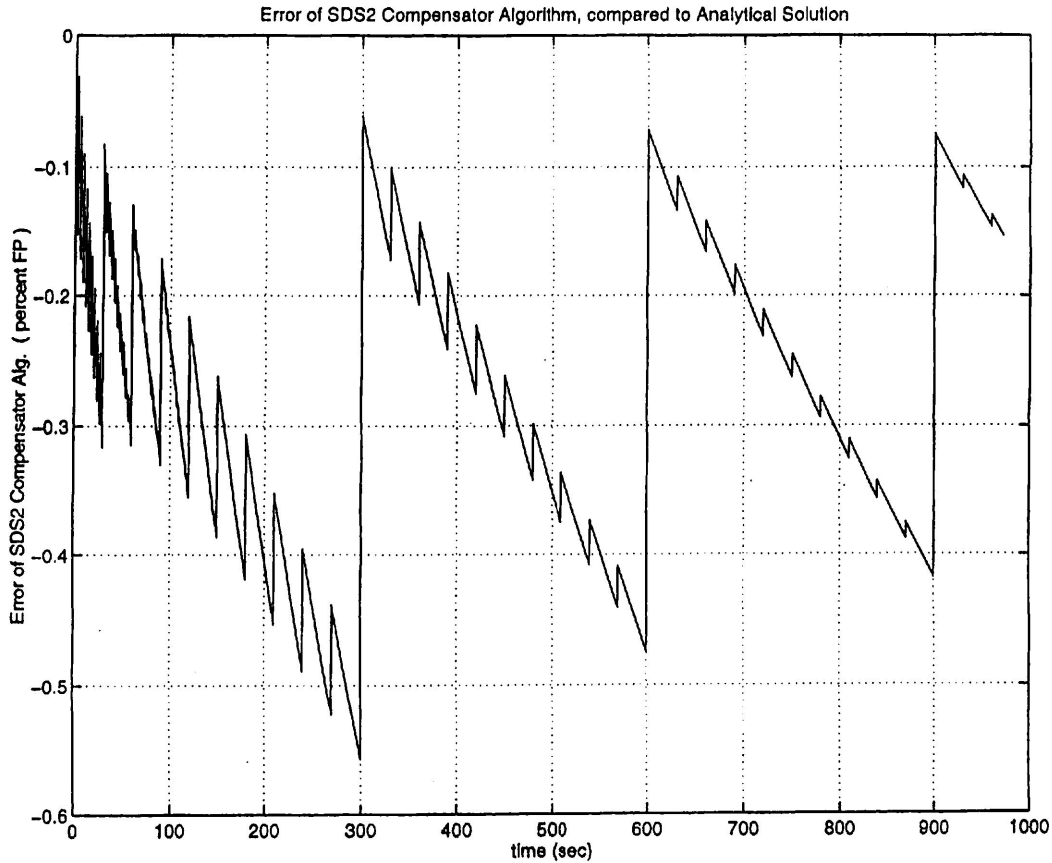


Figure 11. Power Step from 0 %FP to 126 %FP at  $t_0 = 0$

### 3.3 Effect of Timing of the First Simultaneous Compensating Action

The four dynamic compensating terms  $C\_alg_j$ ,  $j = 1, \dots, 4$  are triggered periodically into action by the trip computer timers, with sampling times  $\Delta t_j$ ,  $j = 1, \dots, 4$  specified in Table 1. Because the timers are synchronized, every 3000 sec the four terms  $C\_alg_j$  are triggered simultaneously. As discussed in Section 2.5, for the **fast changes** in neutronic power the moment  $t_{act}$  of occurrence of the **first simultaneous compensating action** (FSCA) by the four terms, with respect to the initiation moment  $t_0$  of the neutronic power  $\Theta_{NP}(t)$  change, considerably affects the magnitude and sign of compensator's error transient  $\epsilon(t)$ .

For **ramp-type** changes in neutronic power the effect of timing of the FSCA on the resulting numerical compensator error is negligible, even for cases with the fastest ramp rates of 126 %FP/hr, as in the Case (a). Such a rate is relatively slow, when compared with the abrupt, step-type changes. Therefore, at time  $t_{act}$  when the FSCA occurs (in our simulations  $t_{act} = 0.3$  sec), the initial increase in detector reading  $Dt_i(t_k)$  (relative to its initial steady state value at  $t_0 = 0$ ) is very small.

Accordingly, the driving terms  $\frac{\Delta t_j}{\tau_{1j} + \Delta t_j} \cdot A_{1j} \cdot Dt_i(t_k)$ ,  $j = 1, \dots, 4$ , in Eqs.(5) are even smaller (by two orders of magnitude, or more), particularly for the two slowest terms  $C\_alg_3$  and  $C\_alg_4$ , with the largest time constants of  $\tau_3 = 2400$  sec and  $\tau_4 = 300,000$  sec. In the next (smallest) sampling time  $t_1 = t_{act} + \Delta t_1 = 3.3$  sec only the fastest term  $C\_alg_1$  is triggered into action (for the second time) and then recomputed every 3 sec. From that time on, i.e. for  $t \geq t_1$  the system acts exactly as described in the Case (a). Namely, the four compensating terms are triggered **sequentially**, with the second term  $C\_alg_2$  calculated (second time) at  $t_2 = t_{act} + \Delta t_2 = 30.3$  sec and then every 30 sec, etc. At time  $t_4$  the four dynamic terms act again simultaneously and the whole cycle repeats periodically with 3000 sec period. As a result, and the transients of the overall compensator actions and the resulting error transients are

practically identical to those shown in Case (a). Detailed simulation results for the ramp cases are given in Ref.5.

For **step-type** changes in neutronic power the effect of FSCA timing on the compensator numerical error is discussed below for the most critical case of step-type power increase from 0% to 126% FP.

**Case (g): Step-type Increase in Neutronic Power from 0% FP to 126 %FP, with the Four Compensator Timers Set to Trigger their FSCA just after the Power Step Initiation.**

Parameters of the step increase in neutronic power  $\Theta_{NP}(t)$  in this case are the same as those in Case (f), namely:

$$\begin{aligned} t_0 &= 0 = \text{initial time ;} & T &= 5400 \text{ sec} = \text{duration of the simulation transient ;} \\ b_0 &= 0 \text{ FP} = \text{initial power level ;} & b &= 1.26 \text{ FP} = \text{final power level.} \end{aligned}$$

The reactor is initially at steady state, at zero power level  $b_0 = 0$  FP. Accordingly, the initial conditions imposed on the dynamic compensating terms  $C_j$  and  $C_{alg_j}$  are set to zero, and the resulting compensated detector initial responses are also zero.

At the initial moment  $t_0$  the detector reading  $Dt_i(t_0)$  undergoes an instantaneous increase from 0 %FP all the way up to the SDS2 NOP trip setpoint of 126 %FP. However, in contrast to Case (f), the four compensator timers are set to trigger their FSCA immediately after the initiation of the power step, that is at the first action time  $t_{act} = t_0 + \Delta t = 0.3$  sec.

At time  $t_{act}$  the four driving terms  $\frac{\Delta t_j}{\tau_{1j} + \Delta t_j} \cdot A_{1j} \cdot Dt_i(t_k)$ ,  $j = 1, \dots, 4$ ; in the numerical algorithm (5) act simultaneously, with the sampling time intervals  $\Delta t_j$  set permanently to values given in Table 1, Section 2.2, rather than to be set to 0.3 sec (only for this first time moment) to ensure the proper operation of the backward finite difference algorithm. Combined with the full momentary increase in  $Dt_i$ , the resulting first simultaneous increase in the four driving terms  $\frac{\Delta t_j}{\tau_{1j} + \Delta t_j} \cdot A_{1j} \cdot Dt_i(t_1)$  is much larger than expected, as explained in Section 2.5. It yields a momentary excessive increase in the four compensating terms  $C_{alg_{ij}}(t_{act})$ ,  $j = 1, \dots, 4$ ; and their sum  $SC_{alg_i}(t_{act})$ , much larger than in Case (a), producing a substantial initial compensating pulse. As a result, the numerical compensator initially **overcompensates** (in negative direction) the detector response, and the initial value of the error  $\epsilon(t)$  may even reverse its sign. From that time on, for  $t \geq t_{act}$  the system acts exactly as described in Case (f), i.e. the four compensating terms are triggered sequentially, in the same manner as in the Case (f), as explained before.

The simulated error transient  $\epsilon(t)$  for this case is shown in Fig.12, in units of fraction of %FP. The transients of the individual compensating terms  $C_{alg_{ij}}$  and their sum  $SC_{alg_i}$  are displayed in Fig.13. For better illustration, the first 1000 sec of the error transient is shown in Fig.14. The effect of timing of the FSCA is clearly visible. More detailed simulation results are described in Ref.5.

The largest short term error  $STE(t)$  is about **thirty percent** larger in magnitude than in Case (f) and the polarity of the error has been **reversed** from negative to positive, due to the overcompensating effect of FSCA, as explained before. The largest  $STE(t)$  occurs immediately after the transient initiation, triggered by the FSCA. The long-term error is smaller than in Case (f).

The maximum (in magnitude) short and long-term errors, based on transients from Figs.14 and 12 are correspondingly

$$\begin{aligned} \max [ STE(t) ] &\approx 0.73 \text{ \%FP, occurring at } t_{act} = t_0 + \Delta t = 0.3 \text{ sec. into the transient;} \\ \max [ LTE(t) ] &\approx 0.40 \text{ \%FP, occurring at 300 sec into the transient.} \end{aligned}$$

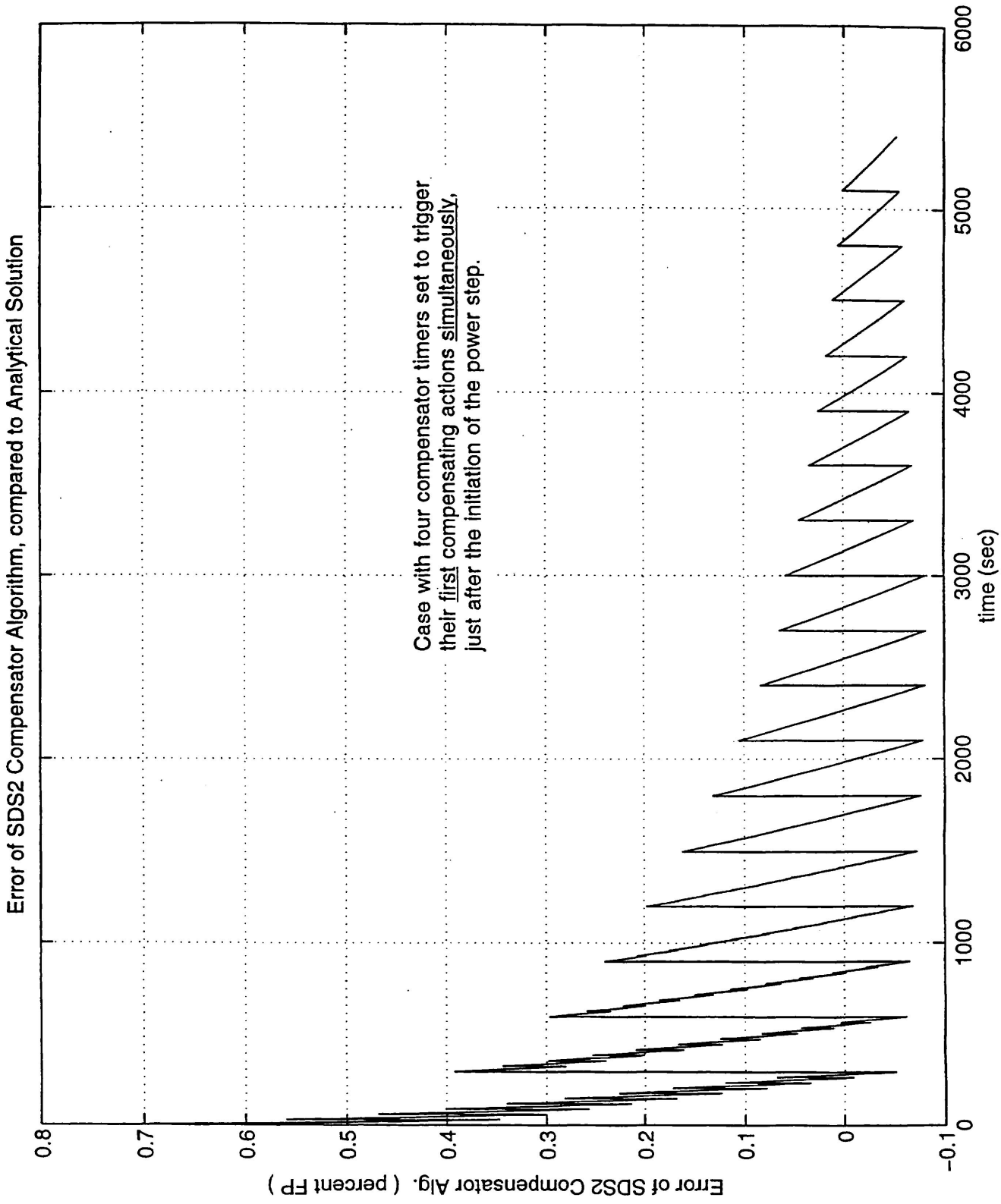


Figure 12. Power Step from 0 %FP to 126 %FP at t0 = 0

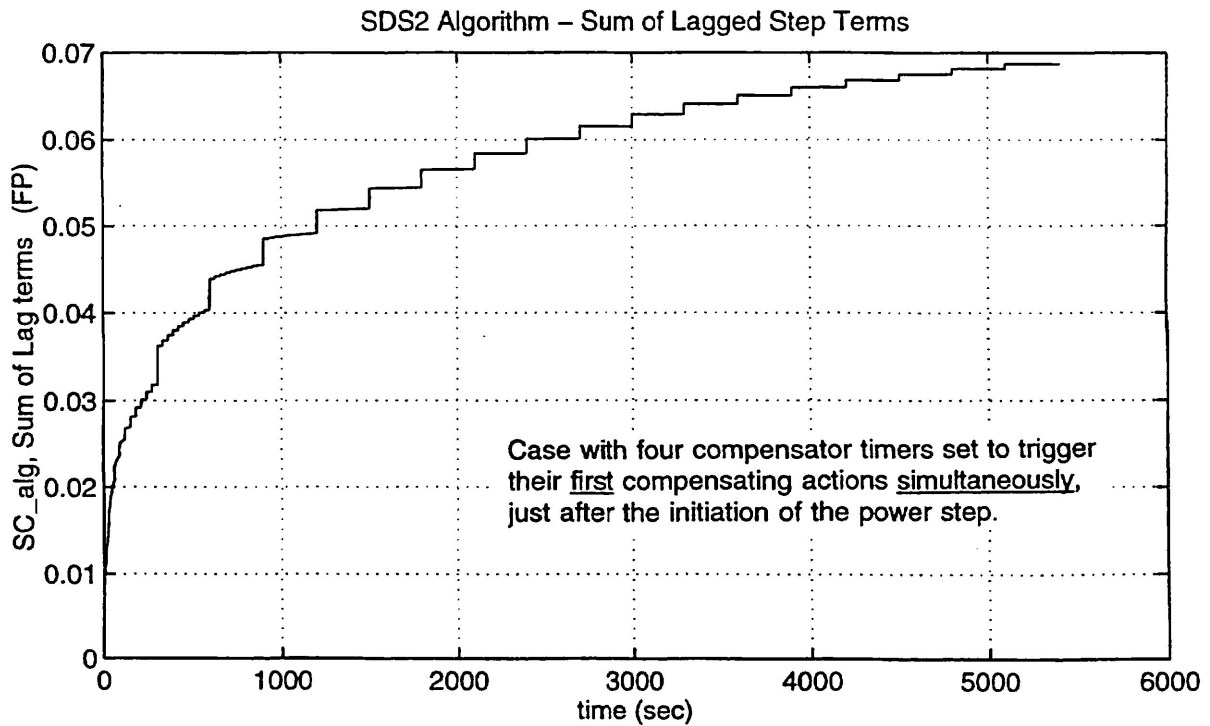
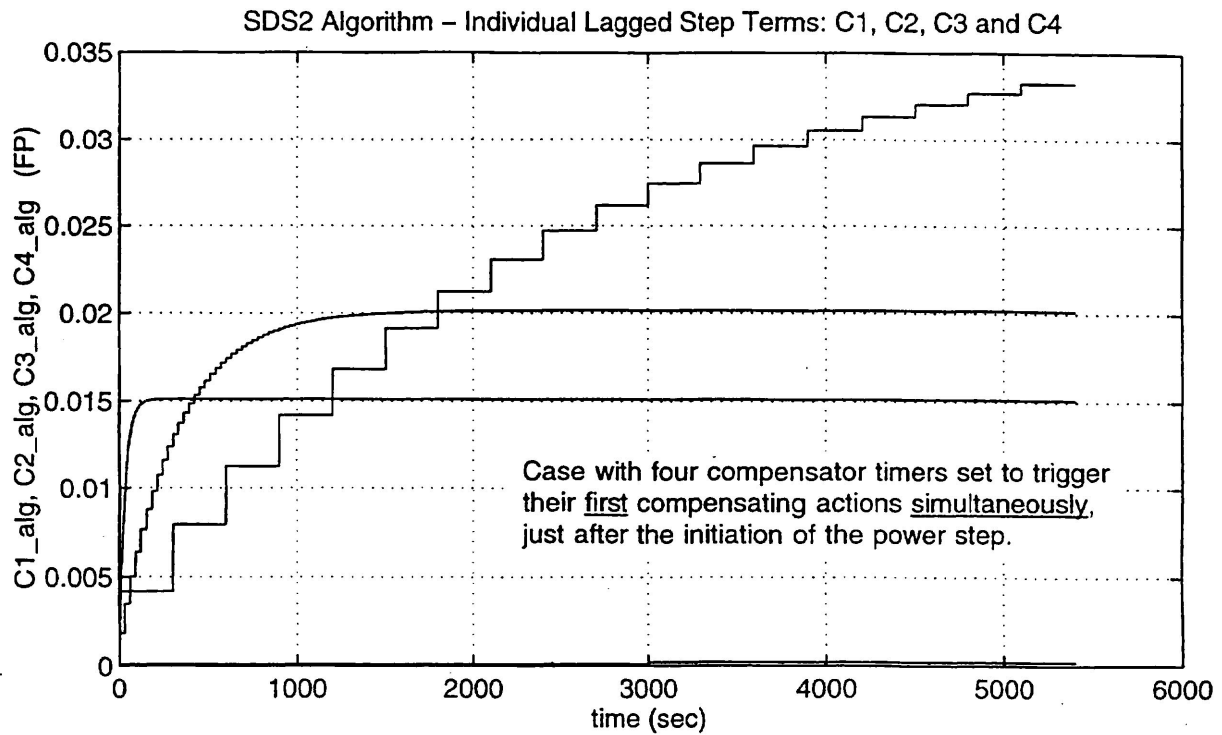


Figure 13. Power Step from 0 %FP to 126 %FP at  $t_0 = 0$

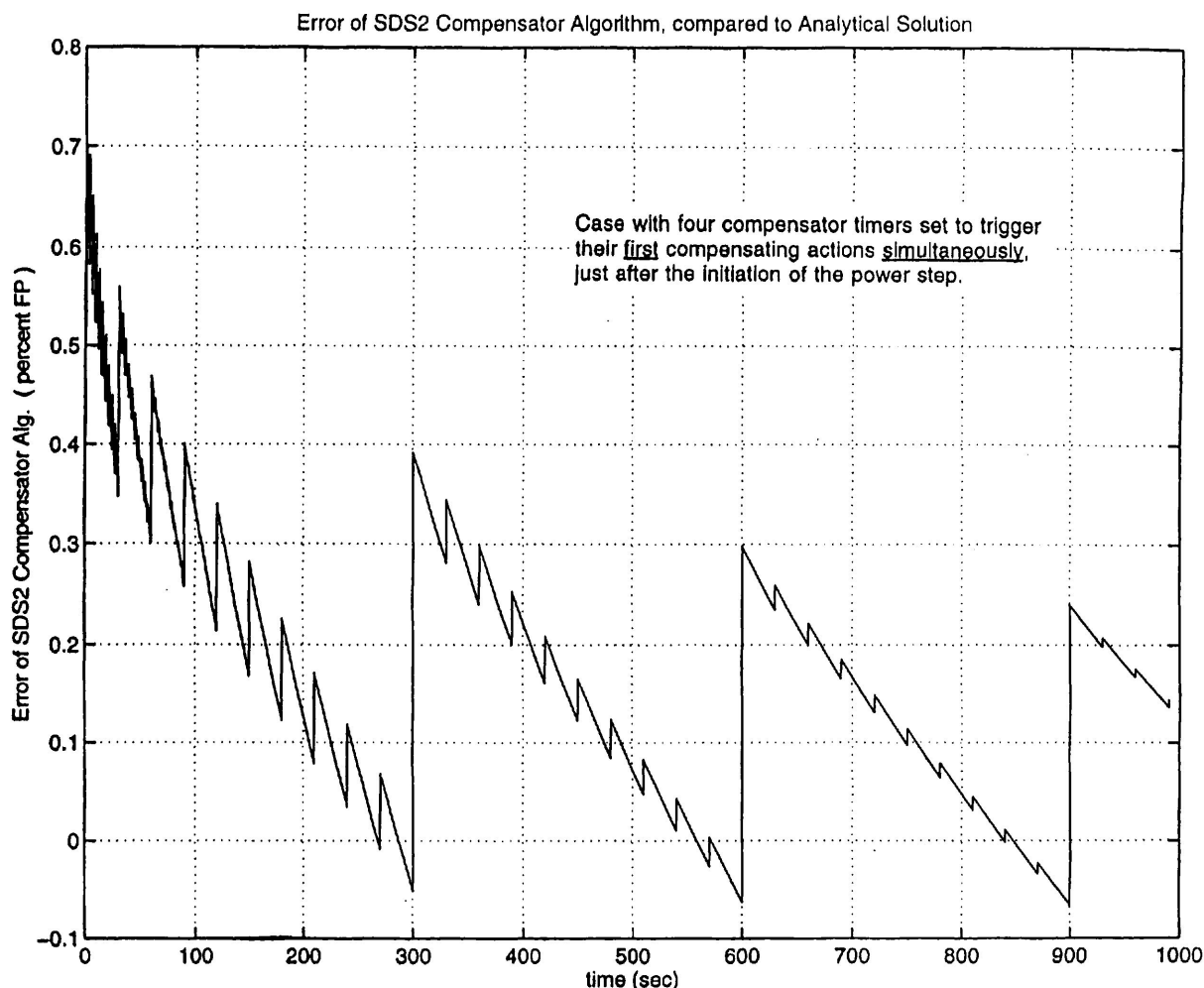


Figure 14. Power Step from 0 %FP to 126 %FP at  $t_0 = 0$

#### 4. Conclusions

Analysis of the NOP detector compensator error  $\epsilon(t)$  caused by the numerical compensation algorithm implemented in SDS2 trip computers was carried out for the specified family of neutronic power variations, as requested by and agreed upon with Darlington NGD. The family of neutronic power transients used in the analysis is specified at the beginning of Section 3. The main simulation results and the relevant analysis are described in Section 3. The results indicate that the most limiting are the cases with large step-type increase in neutronic power, from 0 %FP up to the SDS2-NOP trip setpoint of 126 %FP, as expected. In particular, for the short-term error (up to 300 sec transient time) the most limiting is the Case (g), with the FSCA occurring immediately after the power step initiation. For the long-term error (above 300 sec time) the most limiting is the Case (f), with the sequential mode of action, when the FSCA of the four compensating terms occurs 3000 sec after the power step initiation.

Cases with large step power reductions can be related to failures in the SDS2 system hardware. For example, in case of a sudden loss of the 120 V ac power supply to the NOP detector amplifiers, with reactor operating at full power, the uncompensated detector signal (represented by  $D_t$  in the compensation algorithm (5)) will momentarily drop from the 100 %FP level to 0 %FP. In such a scenario the resulting compensator short-term error transient will be bounded by the analysis carried out for Case (g), and the long-term error will be bounded by the analysis carried out for Case (f). The remaining cases with smaller power increase or power reduction yield smaller numerical error  $\epsilon(t)$ . Cases with ramp power variations are apparently less limiting, but represent more realistic scenarios of variations in reactor power.

The maximum (in magnitude) short and long-term errors, based on analysis of Cases (g) and (f) are:

$$\max [ \text{STE}(t) ] \approx 0.73 \% \text{FP}, \quad \text{and} \quad \max [ \text{LTE}(t) ] \approx -0.47 \% \text{FP}.$$

As explained in Section 2.5 on Methodology, the relative timing of the FSCA by the four dynamic compensating terms varies randomly within a time range from 0 to 3000 sec, i.e. it is a truncated random variable with a uniform probability distribution. Hence, the resulting numerical compensator error  $\epsilon(t)$  is a random process, which realizations (trajectories) are constrained within a region (envelope) defined by the enlisted maximum short and long-term errors.

The resulting short and long-term error limiting envelopes, bounding for all the cases specified in the list of the simulated power transients are :

$$\begin{aligned} \text{Short-term envelope} &= \pm 0.75 \% \text{FP}, \quad \text{defined for } 0 \leq t \leq 300 \text{ sec;} \\ \text{Long-term envelope} &= \pm 0.50 \% \text{FP}, \quad \text{defined for } t > 300 \text{ sec.} \end{aligned}$$

## 5. References

1. N.H. Drewell, I.L. McIntyre: *Dynamic Response of Bruce B Prototype Self-Powered Flux Detectors in NRU*, Rep. No. CRNL-2776, Chalk River Nuclear Laboratories, Chalk River, Ontario, January 1985.
2. J.G. Sutherland: *SDS2 Trip Computer Functional Specification*, OH DNGD TSB-3D2, PSS-38-68300-001, AECL January 28, 1992.
3. *DNGD Shutdown System Trip Computer Software Redesign Project, Trip Computer Design Requirements (TCDR)*, Ontario Hydro Document NK38-DID-68300-001-R0, September 27, 1995.
4. *DNGD Shutdown System Trip Computer Software Redesign Project, SDS2 Trip Computer Design Description (TCDD)*, Ontario Hydro Document NK38-DID-68300-002-R00, November 6, 1996.
5. A.P. Firla: Darlington NGD: *Numerical Compensation of NOP Detectors in SDS2 Trip Computers*, OH Report No. 975118, Rev.0, Ontario Hydro Nuclear, October 1997.
6. A.P. Firla, B.C. Choy, K.C. Ng: *Trip Parameter Assessment, Darlington NGS*, OH Report No. 86160, Ontario Hydro-NSSD, May 1987.
8. Ch.L. Phillips, R.D. Harbor: *Feedback Control Systems*, 3-rd Edition, Prentice Hall, Englewood Cliffs, NJ, 1996.
9. R. Fratila (ed.), *Theory of Linear Systems*, REA Research and Education Association, New York 1982.
10. W.H. Press, B.P. Flannery, S.A. Teukolsky, W.T. Vetterling, *Numerical Recipes - The Art of Scientific Computing*, Cambridge University Press, New York 1987.
11. S. Nakamura: *Numerical Analysis and Graphic Visualization with MATLAB*, Prentice Hall PTR, Upper Saddle River, NJ, 1996.
12. *MATLAB, High-Performance Numeric Computation and Visualization Software*, The Math Works, Inc., Natick, Massachusetts, July 1993.

## APPENDIX A: Derivation of Numerical Algorithm Used in SDS2 NOP Detector Compensation

The numerical compensation algorithm (5) is obtained by numerically integrating the differential equations in system (4) describing the dynamic terms  $C_j(t)$ ,  $j = 1, \dots, 4$  and time-discretizing the remaining algebraic equations. The first order backward Euler method is used, with discrete time  $t = t_k$  and fixed time step  $\Delta t = t_k - t_{k-1}$ .

The first order backward difference for the derivatives in differential eqs.(4) is defined (see e.g. Refs.10), as  $\frac{dx(t_k)}{dt} \approx \frac{x(t_k) - x(t_{k-1})}{\Delta t}$ . The order of accuracy of the first order backward Euler method is the same as that of the forward one. However, the backward method has two significant advantages (see Refs.10 and 11), namely: (\*) it is unconditionally stable, and (\*\*) positivity of solution is guaranteed when the solution is supposed to be positive.

For simplicity, let's denote

$$C_j(t) = C_j(t_k) = C_j(k), \quad C_j(t - \Delta t_j) = C_j(t_{k-1}) = C_j(k-1), \quad C_j(t + \Delta t_j) = C_j(t_{k+1}) = C_j(k+1);$$

and  $Dt(t_k) = Dt(k)$ ,  $j = 1, \dots, 4$ ; where  $\Delta t_j =$  sampling time for the  $j^{\text{th}}$  lag term loop.

Using the simplified notation, the backward difference of  $C_j(t)$  becomes

$$\frac{dC_j(t_k)}{dt} \approx \frac{C_j(t_k) - C_j(t_k - \Delta t_j)}{\Delta t_j} = \frac{C_j(k) - C_j(k-1)}{\Delta t_j}, \quad j = 1, \dots, 4; \quad (\text{A1})$$

Substituting the backward difference (A1) into differential equations (4) we obtain

$$\frac{C_j(k) - C_j(k-1)}{\Delta t_j} + \frac{1}{\tau_j} \cdot C_j(k) = \frac{A_j}{\tau_j} \cdot Dt(k), \quad k = 1, 2, \dots; \quad j = 1, \dots, 4;$$

Grouping the terms  $C_j(k)$  on the LHS of the equation and multiplying both sides by  $\frac{\tau_j}{(\tau_j + \Delta t_j)}$  we get

$$C_j(k) = C_j(k-1) \cdot \frac{\tau_j}{(\tau_j + \Delta t_j)} + A_j \cdot \frac{\Delta t_j}{(\tau_j + \Delta t_j)} \cdot Dt(k);$$

Adding and subtracting  $C_j(k-1)$  to the right-hand side of the equation, yields

$$C_j(k) = C_j(k-1) + \frac{\tau_j \cdot C_j(k-1) - (\tau_j + \Delta t_j) \cdot C_j(k-1)}{\tau_j + \Delta t_j} + \frac{\Delta t_j}{\tau_j + \Delta t_j} \cdot A_j \cdot Dt(k);$$

The two terms  $\tau_j C_j(k-1)$  cancel and we finally obtain

$$C_j(k) = C_j(k-1) + \frac{\Delta t_j}{\tau_j + \Delta t_j} \cdot \left[ A_j \cdot Dt(k) - C_j(k-1) \right]; \quad k = 1, 2, \dots; \quad (\text{A2})$$

$j = 1, \dots, 4;$

which, after using full notation and substituting  $C_j(k) = C_{\text{alg } ij}(t_k)$ ,  $Dt(k) = Dt_i(t_k)$ ,  $A_j = A_{ij}$  and  $\tau_j = \tau_{ij}$  for the  $i^{\text{th}}$  generic detector, becomes the first equation of the numerical algorithm (5).

The initial conditions are set in the manner discussed in Section 2.4, namely  $C_{\text{alg } ij}(t_0) = C_{ij}^0 = A_{ij} \cdot b$ ,  $t_0 = 0$ ;  $j = 1, \dots, 4$ ;  $i = 1, 2, \dots, 17$ .

Substituting discrete variables  $SC_{\text{alg } ij}(t_k)$  for  $SC(t)$  and  $DtCmp_{\text{alg } i}(t_k)$  for  $DtCmp(t)$  in the algebraic equations of model (4), we immediately obtain the last two equations of algorithm (5).

The simulation results presented in Section 3 show that the compensated detector responses calculated using the numerical algorithm (5) closely resemble their corresponding analytical solutions.

## APPENDIX B: Derivation of Analytical Solution for Compensator Model with Bounded Ramp-type Changes in Neutronic Power

Bounded ramp-type variations in neutronic power  $\Theta_{NP}(t)$  are specified by relation (8) as

$$\Theta_{NP}(t) = \begin{cases} (a \cdot t + b), & \text{for } 0 \leq t < t_1; \\ D, & \text{for } t \geq t_1; \end{cases}$$

where:  $b$  = initial reactor power level ,  
 $a$  = rate of power increase ,  
 $D$  = final reactor power level ,  
 $t_1$  = end time for the ramp driving force .

To derive the analytical solution (9), one has to solve the set of linear differential equations in the compensator differential model (4). The equations describe dynamics of the lag terms  $C_j, j = 1, \dots, 4$ ; and are of form

$$\begin{aligned} \frac{dC_j(t)}{dt} &= -\frac{1}{\tau_j} \cdot C_j(t) + \frac{A_j}{\tau_j} \cdot Dt(t), \quad j = 1, \dots, 4; \\ C_j(t_0) &= C_j^0 \text{ are initial conds., } t_0 = 0; \end{aligned} \quad (B1)$$

where:  $Dt(t) = \Theta_{NP}(t)$  = equation's driving force,  $t \geq 0$ .

The solution is found using a state-space solution (see e.g. Ref.8 or 9). For a general system of a linear, vector differential equation  $\frac{dx}{dt} = A \cdot x(t) + f(t)$ ,  $x(t_0) = x_0$ ,  $t \geq t_0$ ; the state solution is of form

$$x(t) = \Phi(t-t_0) \cdot x(t_0) + \int_{t_0}^t \Phi(t-s) \cdot f(s) ds, \quad t \geq t_0; \quad (B2)$$

where  $\Phi(t-t_0) = e^{A \cdot (t-t_0)}$  is the system's state transition matrix, and  $A$  is a matrix of system coefficients adjacent to  $x(t)$ . The system of equations (B1) is decoupled and they all have identical form. Therefore, we can seek the solution of a single, scalar equation for a generic compensating term  $C_j$ . Hence, the state transition matrix  $\Phi(t-t_0)$ , driving force  $f(t)$  and initial condition  $x(t_0)$  are scalars of the form

$$\Phi(t-t_0) = e^{-\frac{(t-t_0)}{\tau_j}}, \quad f(t) = \frac{A_j}{\tau_j} \cdot \Theta_{NP}(t), \quad x(t_0) = C_j(t_0) = C_j^0, \quad t_0 = 0;$$

Accordingly, a general solution for the generic term  $C_j$  becomes

$$C_j(t) = e^{-\frac{t}{\tau_j}} \cdot C_j(0) + \frac{A_j}{\tau_j} \int_0^t e^{-\frac{(t-s)}{\tau_j}} \cdot \Theta_{NP}(s) ds, \quad C_j(0) = C_j^0, \quad t \geq 0; \quad (B3)$$

First, lets find the solution  $C_j(t)$  to an **unbounded** ramp  $\Theta_{NP}(t)$ . Substituting  $\Theta_{NP}(t) = a \cdot t + b$  into Eq.(B3), the integral in the RHS becomes

$$\frac{A_j}{\tau_j} \int_0^t e^{-\frac{(t-s)}{\tau_j}} \cdot \Theta_{NP}(s) ds = \frac{A_j}{\tau_j} \left[ a \int_0^t e^{-\frac{(s-t)}{\tau_j}} \cdot s ds + b \int_0^t e^{-\frac{(s-t)}{\tau_j}} ds \right]; \quad (B4)$$

The first integral in the RHS is a convolution integral and can be integrated by parts, to get after

few transformations  $\int_0^t e^{-\frac{(s-t)}{\tau_j}} \cdot s ds = \tau_j \left[ t - \tau_j \cdot (1 - e^{-\frac{t}{\tau_j}}) \right]$ . The second integral in the RHS

is obviously  $\int_0^t e^{-\frac{(s-t)}{\tau_j}} ds = \tau_j \cdot e^{-\frac{(s-t)}{\tau_j}} \Big|_{s=t} - \tau_j \cdot e^{-\frac{(s-t)}{\tau_j}} \Big|_{s=0} = \tau_j \left[ 1 - e^{-\frac{t}{\tau_j}} \right]$ .

Substituting both relations back into Eq.(B3) we get

$$C_j(t) = e^{-\frac{t}{\tau_j}} \cdot C_j^0 + A_j \left( a \left[ t - \tau_j \cdot (1 - e^{-\frac{t}{\tau_j}}) \right] + b \left[ 1 - e^{-\frac{t}{\tau_j}} \right] \right), \quad t \geq t_0;$$

and, after re-grouping we obtain the solution for the unbounded ramp  $\Theta_{NP}(t)$ , in the form

$$C_j(t) = A_j \left( b + a \left[ t - \tau_j \cdot (1 - e^{-\frac{t}{\tau_j}}) \right] \right) - \left[ A_j \cdot b - C_j^0 \right] \cdot e^{-\frac{t}{\tau_j}}; \quad (B5)$$

$$C_j^0 = C_j(0) = \text{initial condition}, \quad t \geq 0;$$

The solution (B5) is valid for any  $t \geq 0$ , and hence for the duration of the unbounded ramp  $0 \leq t \leq t_1$ .

Now, let's find the solution for the bounded part of the  $\Theta_{NP}(t)$  ramp, which is the second part of our transient, with the time range  $t_1 \leq t \leq +\infty$ . We again utilize the state-space solution (B2), but now for  $t \geq t_1$ , with the new initial condition defined at  $t_0 = t_1$ :  $x(t_0) = C_j(t_1)$ . This new initial condition is given by the solution (B5) at  $t = t_1$ . Accordingly, we substitute now

$$\Phi(t-t_0) = e^{-\frac{(t-t_1)}{\tau_j}}, \quad f(t) = \frac{A_j \cdot D}{\tau_j}, \quad x(t_0) = C_j(t_1), \quad t_0 = t_1 = \text{new initial time};$$

in the state solution (B2), and it follows that the general solution for term  $C_j$  in the time range  $t \geq t_1$  becomes

$$C_j(t) = e^{-\frac{(t-t_1)}{\tau_j}} \cdot C_j(t_1) + \frac{A_j \cdot D}{\tau_j} \int_{t_1}^t e^{-\frac{(t-s)}{\tau_j}} ds, \quad t \geq t_1; \quad (B6)$$

The integral in the RHS is calculated (in a similar manner as before) to get

$$\int_{t_1}^t e^{-\frac{(t-s)}{\tau_j}} ds = \tau_j \left[ 1 - e^{-\frac{(t-t_1)}{\tau_j}} \right]$$

and the solution  $C_j(t)$  for  $t \geq t_1$  (the bounded part of the transient) becomes

$$C_j(t) = e^{-\frac{(t-t_1)}{\tau_j}} \cdot C_j(t_1) + A_j \cdot D \left[ 1 - e^{-\frac{(t-t_1)}{\tau_j}} \right] = A_j \cdot D - \left[ A_j \cdot D - C_j(t_1) \right] \cdot e^{-\frac{(t-t_1)}{\tau_j}}; \quad (B7)$$

$t \geq t_1$

where  $C_j(t_1)$  is known from the solution (B5) at  $t = t_1$ . Joining together solutions (B5) and (B7) we finally obtain the global solution  $C_j(t)$ ,  $j = 1, \dots, 4$ ; for  $t \geq 0$  in the form

$$C_j(t) = \begin{cases} A_j \cdot \{ b + a \cdot [ t - \tau_j \cdot (1 - e^{-\frac{t}{\tau_j}}) ] \} - [ A_j \cdot b - C_j^0 ] \cdot e^{-\frac{t}{\tau_j}}, & \text{for } 0 \leq t < t_1; \\ A_j \cdot D - [ A_j \cdot D - C_j(t_1) ] \cdot e^{-\frac{(t-t_1)}{\tau_j}}, & \text{for } t \geq t_1; \end{cases} \quad (B8)$$

$$C_j(0) = C_j(t=0) = C_j^0 = \text{overall initial conditions}, \quad j = 1, \dots, 4;$$

which is the main part of the analytical solution (9). The initial conditions in Eq.(9) have been set to  $C_j^0 = A_j \cdot b$ , as discussed in Section 2.4, but the global solution is valid for any initial conditions  $C_j^0$ .

The remaining two algebraic relations in the analytical solution (9), describing  $SC(t)$  and  $DtCmp(t)$  are the same as in the compensator's differential model (4).

The rate of change of the analytical solution,  $\frac{d}{dt} DtCmp(t)$ , is calculated as follows.

First, we calculate the rate  $\frac{dC_j}{dt}$ , which for the global solution is

$$\begin{aligned}\frac{dC_j}{dt} &= A_j \cdot a \left[ 1 - \tau_j \cdot \left( e^{-\frac{t}{\tau_j}} \cdot \frac{1}{\tau_j} \right) \right] + \frac{1}{\tau_j} [A_j b - C_j^0] \cdot e^{-\frac{t}{\tau_j}} \\ &= A_j \cdot a \left[ 1 - e^{-\frac{t}{\tau_j}} \right] + \frac{1}{\tau_j} [A_j b - C_j^0] \cdot e^{-\frac{t}{\tau_j}}, \quad \text{for } 0 \leq t < t_1;\end{aligned}$$

and

$$\frac{dC_j}{dt} = -[A_j \cdot D - C_j(t_1)] \cdot \frac{d}{dt} \left( e^{-\frac{(t-t_1)}{\tau_j}} \right) = [C_j(t_1) - A_j \cdot D] \cdot \frac{1}{\tau_j} \cdot e^{-\frac{(t-t_1)}{\tau_j}}, \quad \text{for } t \geq t_1;$$

Using the initial conditions  $C_j^0 = A_j b$  we get

$$\frac{dC_j}{dt} = A_j \cdot a \left[ 1 - e^{-\frac{t}{\tau_j}} \right], \quad \text{for } 0 \leq t < t_1, \quad \text{and} \quad \frac{dC_j}{dt} = [C_j(t_1) - A_j \cdot D] \cdot \frac{1}{\tau_j} \cdot e^{-\frac{(t-t_1)}{\tau_j}}, \quad \text{for } t \geq t_1;$$

At  $t = 0$ , the rate  $\frac{dC_j}{dt} = 0$ , which is consistent with the assumption (A3) in Section 2.1.

For very large  $t_1$  and very large  $t$ , but such that  $t < t_1$ , with  $t \rightarrow +\infty$  we have  $\frac{dC_j}{dt} \rightarrow A_j \cdot a$ , as expected.

Accordingly, for  $0 \leq t < t_1$ , i.e. for the unbounded part of the ramp transient the rates of change of the

sum  $SC(t)$  and the compensated detector response  $DtCmp(t)$ , are  $\frac{dSC}{dt} = \sum_{j=1}^4 A_j \cdot a \left[ 1 - e^{-\frac{t}{\tau_j}} \right]$  and

$$\frac{d}{dt} DtCmp(t) = \left( 1 + \sum_{j=1}^4 A_j \right) \cdot \frac{d\Theta_{NP}}{dt} - \frac{dSC}{dt} = \left( 1 + \sum_{j=1}^4 A_j \right) \cdot a - \sum_{j=1}^4 A_j \cdot a \left[ 1 - e^{-\frac{t}{\tau_j}} \right] = a \cdot \left( 1 + \sum_{j=1}^4 A_j e^{-\frac{t}{\tau_j}} \right).$$

For very large  $t_1$ , with  $t \rightarrow +\infty$ , we have  $\frac{d}{dt} DtCmp(t) \rightarrow a$ , i.e. the rate of the compensated detector response approaches the rate of neutronic power ramp.

For  $t \geq t_1$ , the rate of change of the sum  $SC(t)$  becomes

$$\frac{dSC}{dt} = \sum_{j=1}^4 \frac{dC_j}{dt} = \sum_{j=1}^4 [C_j(t_1) - A_j \cdot D] \cdot \frac{1}{\tau_j} \cdot e^{-\frac{(t-t_1)}{\tau_j}};$$

Correspondingly, the rate of the compensated detector response  $DtCmp(t)$  becomes

$$\frac{d}{dt} DtCmp(t) = \left( 1 + \sum_{j=1}^4 A_j \right) \cdot \frac{d\Theta_{NP}}{dt} - \frac{dSC}{dt} = \left( 1 + \sum_{j=1}^4 A_j \right) \cdot \frac{dD}{dt} - \frac{dSC}{dt} = \sum_{j=1}^4 [A_j \cdot D - C_j(t_1)] \cdot \frac{1}{\tau_j} \cdot e^{-\frac{(t-t_1)}{\tau_j}}.$$

It implies that with  $t \rightarrow +\infty$ ,  $\frac{d}{dt} DtCmp(t) \rightarrow 0$ , i.e. the rate of the compensated detector response approaches zero, as it should.

## Author Index

Author	Session(s)	Author	Session(s)	Author	Session(s)
Al-Basha, H.S.	2C	Csullog, G. W.	2A, 2A	Haynes, M.	Plenary
Allsop, P.J.	3B	Czuppon, G.	3A	Hejzlar, P.	1C, 1C
Andrei, V.	2A	Daigneault, M.	5A	Hernu, P.	2D
Andseta, S.	2B	Davey, E.	3D, 3D, 3D, 3D	Herzog, K.	3D
Arapakota, D.	1C	Davies, K.	1C	Hoffarth, B.E.	5A
Ardeshiri, F.	4C	Davis, M.W.	4A	Holtorp, J.	3B
Arsenault, B.	4C	Debos, E.	2C	Hotte, G.	4B
Artiss, W.G.	3D	Delorme, G.	3C	Howard, S.	3D
Aryono, N.A.	1C, 1C	De Verne, M.	3D	Hulley, V.R.	2A
Auverlot, D.	1A	Diaconu, Gh.	2D	Humphries, J.R.	1C
Aydogdu, K.	4C	Diamond, W.T.	5B	Huynh, H.M.	4D
Bailey, C.	2D	Dickson, L.W.	5C	Idvorian, N.	5B
Balasoiu, M.	2A	Didsbury, R.	3D	Irish, J.D.	5C
Banas, A.O.	2D	Dinadis, N.	4B	Ishikawa, H.	1A
Basso, R.	3D, 3D	Dixon, D.	2A	Janzen, V.P.	4D
Baudouin, A.	3C, 4B	Donnelly, J.V.	4C	Jarrell, J.P.	2B
Bayoumi, M.H.	5B	Dormuth, D.	1B	Jee, K.K.	4B
Bellil, A.	2D	Driscoll, M.J.	1C, 1C	Johansen, K.	2B
Bennett, L.G.I.	3A, 5A	Duffey, R.B.	Plenary, 2B	Johnson, H.M.	4A
Beuthe, T.G.	1B, 1B	Duport, P.	4A	Jones, T.A.	5A
Bilanovic, Z.	3C	Edwards, N.W.	2A, 2A	Jonckheere, M.G.	5C
Bond, J.	Plenary	Evans, D.	3B	Joseph, R.	2A
Bonin, H.W.	3C	Feher, M.	3D	Judd, R.	3D
Boubcher, M.	2C	Firla, A.P.	3A	Kapoor, K.	3A
Bourque, L.R.	5C	Fitzgerald, W.R.	2B	Kaveh, S.	4C
Bradley, M.	3D	Fluke, R.	4B	Kennedy, G.	5A
Brisson, J.R.	5A	Garisto, N.C.	4A	Khaloo, R.	5A
Burrill, K.A.	4B	Gentner, N.	4A	Koclas, J.	4C, 4C
Caron, F.	3B	Gerardi, J.L.	4D	Kugler, G.	Plenary
Casota, M.	2D	Gibb, R.A.	4C, 4D, 5C, 5C	Kundurpi, P.S.	5B
Cattrysse, L.F.	2B	Glöckler, O.	3A	Kyle, G.	5C
Chambers, D.B.	4A	Glodeanu, F.	2A	Labrie, J-P.	Plenary
Chamney, L.	2B	Gomes, G.	3A, 3A	Lan, T.H.	2D
Chan, A.M.C.	2D	Gray, M.	2A	Lane, L.	3D, 3D
Chandler, N.	2A	A.R. Green	5A	Lau, J.H.K.	4D
Chapdelaine, C.	5A	Greenstock, C.L.	5A	Laughton, P.J.	4C
Chapman, T.J.	5C	Grondin, D.	2B	Lee, A.G.	Plenary
Chatterton, R.	3D	Gulshani, P.	4D	Lee, B.C.	4B
Cheluget, E.L.	4B	Handbury, J.C.	2D, 3A	Lee, S.M.	4B
Chow, H.C.	3C	Hara, K.	2A	Lee, S.S.	2A
Choy, E.	1C	Hare, M.	1B	Lee, P.Y.C.	5C
Claudi, R.	3B	Hartley, P.	3D	Lei, Q.M.	4D
Collins, W.M.	5C	Hasegawa, H.	1A	Lenghyel, I.	2A
Cooke, D.	3A	Author	Session(s)	Lenton, K.J.	5A
Cornett, R.J.	3B			Lewis, B.J.	3A, 5A
Cournut, A.	2A				
Cousins, T.	3A, 5A				
Craig, S.T.	5C				
Author	Session(s)				

## Author Index (continued)

Author	Session(s)	Author	Session(s)	Author	Session(s)
Lidstone, R.F.	1C	Roy, R.	2C, 4C	White, R.M.	Plenary
Loughead, D.	1B	Rozon, D.	2C, 3C, 3C, 3C	Whitlock, J.J.	1C
Lowe, L.M.	4A			Whynot, T.	2D
Lupton, L.	3D	Sabourin, G.	2A	Wieland, H.K.	3A
		Sancton, R.W.	4D	Wismer, D.A.	3B
Maguire, M.A.	5B	Sandeman, J.	4A	Wong, R.	4B
Mallory, J.P.	1B	Seaborn, B.	1A	Wu, G.J.	2C
Maloney, R.J.	2B	Shen, W.	3C, 3C, 3C	Xing, A.	1C
Mangalaramanan, S.P.	5B	Simanjuntak, A.	5A	Xu, Z.	4D
Manu, C.	4D	Simionov, V.	2A	Yamakawa, M.	1A
Mao, A.C.	3C	Sissaoui, M.T.	2C, 4C	Yaraskavitch, D.	3D
Marleau, G.	2C, 2C, 2C, 2C, 3C, 4C	Smith, B.A.W.	4D	Yang, L.	1B, 4B
		Stebbing, J.D.	3C	Yim, K.	4B
Masuda, S.	1A	Steed, R.G.	4D	Yoon, S.H.	4B, 4B
Mattingly, B.T.	1C	Steward, F.	4B	Young, E.G.	3A
McCann, D.J.	2A	Stewart, M.J.	Plenary		
McCarthy, J.J.	Plenary	Sun, D.	4B	Zikovsky, L.	5A
McGuigan, K.	3D	Sur, B.	3A		
McIntyre, C.	3D				
Metes, M.	2D	Tayal, M.	4D		
Miller, D.G.	4B	Taylor, C.E.	4D		
Miller, M.T.	2A	Taylor, D.	Plenary		
Mitchel, R.E.J.	4A	terHuurne, M.A.	2A, 2A		
Mok, J.I.	5C	Teysseidou, A.	2D		
		Thegerström, C.	1A		
Nash, K.E.	1A	Thompson, J.W.	4C		
Newman, C.W.	3A	Thompson, M.	3D		
		Thompson, M.J.	2B		
Oldaker, I.E.	4D	Thompson, P.	3B		
Osamusali, S.I.	2D	Thompson, P.D.	Plenary		
Osborne, R.V.	4A, 4A	Tillerson, J.	2A		
Ousmoï, M.	5A	Tingle, C.P.	3C		
		Todreas, N.E.	1C, 1C		
Panarella, E.	1C	Torok, J.	3B		
Panesar, D.K.	2A	Tregunno, D.	2B		
Patterson, B.K.	3D	Trivedi, A.	4A		
Pendergast, D.R.	2B, 2B	Tromp, J.H.	4D		
Peplinskie, R.T.	5C	Tsuboya, T.	1A		
Pepper, G.T.	4C	Tume, P.	3A, 5A		
Peryoga, Y.	1C, 1C	Turner, C.W.	4B		
Peters, J.H.	2B				
Petrilli, M.-A.	4B	Umeki, H.	1A		
Pierre, M.	5A				
Pilkington, W.S.	Plenary	Valliant, P.J.	5C		
Pitre, J.	3A	Vecchiarelli, J.	1C		
Popa, A.	2A	Vijayan, S.	3B		
Rao, R.R.	3B	Vu, T.D.	1C		
Reid, M.K.	3A	Wahba, N.N.	5B		
Reid, P.J.	4D, 5C	Whan, T.G.	4D		
Rousseau, K.	2C	Author	Session(s)		
Author	Session(s)				